


Article

Spatial and Temporal Variability in Hydrological Responses of the Upper Blue Nile basin, Ethiopia

Tatenda Lemann ^{1,2,*}, Vincent Roth ^{1,2}, Gete Zeleke ^{1,3}, Alemtsehay Subhatu ^{1,2},
Tibebu Kassawmar ^{2,3} and Hans Hurni ¹

¹ Centre for Development and Environment (CDE) University of Bern, Mittelstrasse 45, 3012 Bern, Switzerland; vincent.roth@cde.unibe.ch (V.R.); gete.z@wlr-eth.org (G.Z.); alemtsehay.teklay.subhatu@cde.unibe.ch (A.S.); Hans.Hurni@cde.unibe.ch (H.H.)

² Integrative Geography—Sustainable Land Management Group, University of Bern, Hallerstrasse 12, 3012 Bern, Switzerland; tibekassa@gmail.com

³ Water and Land Resource Centre, P. O. Box: 3880, 1000 Addis Abeba, Ethiopia

* Correspondence: tatenda.lemann@cde.unibe.ch; Tel.: +41-31-631-88-69

Received: 11 October 2018; Accepted: 13 December 2018; Published: 22 December 2018



Abstract: To assess the spatial and temporal availability of blue and green water for up- and downstream stakeholders, the hydrological responses of the upper Blue Nile basin in the Ethiopian Highlands was modelled and analysed with newly generated input data, such as soil and land use maps. To consider variations in the seasonal climate, topography, soil, land use, and land management, the upper Blue Nile basin was modelled in seven major sub-basins. The modelling showed significant spatial and temporal differences in the hydrological responses of different sub-basins and years. The long-term mean annual drainage ratios of the watersheds range from <0.1 to >0.65, and the annual drainage ratio of one sub-basin can vary from 0.22 to 0.49. Steep slopes, shallow soils, and cultivated areas increase the drainage ratios due to high surface runoff, low soil moisture content, and a smaller share of evapotranspiration. Various climate change scenarios predict more precipitation, and land use change scenarios foresee a higher share of cultivated areas due to population growth. In view of these trends, results from our study suggest that drainage ratios will increase and more available blue water can be expected for downstream stakeholders.

Keywords: hydrological response; hydrological modelling; upper Blue Nile basin; blue and green water

1. Introduction

Most of the water used in the lowlands between Ethiopia and the Mediterranean Sea originates in the Ethiopian Highlands. The Blue Nile basin alone contributes 60%–70% of the water in the River Nile flowing through Sudan and Egypt [1,2]. In Sudan and Egypt, up to 95% of the water used is blue water from the Nile [3]. By contrast, in the headwaters, until recently, more than 95% of the agricultural area was rained, thus using almost exclusively green water [4,5]. Driving forces, such as economic development and population growth, are increasing the demand for water along the entire length of the Nile for food and energy production, and domestic and industrial use. New dams and intensification of agriculture are changing the temporal and spatial use of blue and green water along the Nile, affecting drainage ratios and water availability. Knowledge about the characteristics of different catchments and each catchment's hydrological response is essential to predict the influences of, for example, land use-, irrigation-, and climate change on future spatial and temporal water availability for up- and downstream stakeholders.

In the last few years, various studies were conducted on discharge and precipitation along the upper Blue Nile (Abay) basin. These studies investigated different discharge and precipitation

trends [6,7] or modelled climate change scenarios [8,9], analysed different models with different discharge data from the upper Blue Nile [10–16], and calibrated discharge to model sediment losses along the upper Blue Nile basin [14,17]. Other studies looked at evaporation [18] or different satellite-estimated or measured rainfall data and precipitation distribution in the Blue Nile basin [2,19–21]. However, owing to the scarcity of data and the large size of the upper Blue Nile basin, these studies used a digital elevation model (DEM) with a resolution of 90 m or a higher pixel size and a very general soil and land use map. In addition, most studies incorporated the data of only a few weather stations for a few years in their model and calibrated and validated it with data from one or two gauging stations along the upper Blue Nile Basin. More detailed discharge modelling was conducted by many studies at the catchment level in different watersheds in the upper Blue Nile basin [22–29]. Lemann et al. [30] showed the different hydrological responses to different rainfall patterns and different meteorological conditions in the upper Blue Nile basin, but only at the sub-basin level. Prior to this study, there was no detailed analysis of hydrological responses and discharge simulations over a longer time period at the national basin level, with a soil and land use map of a high spatial resolution and DEM. The heterogeneity of the seasonal climate, topography, soil and land cover, and land management cause big differences in discharge ratios in the Ethiopian Highlands and show the importance of studies with a higher temporal and spatial resolution [30].

The objectives of this study are therefore to generate a detailed overview of the temporal and spatial variations in the drainage ratios over the whole upper Blue Nile basin in the Ethiopian Highlands at the watershed level (mean size 500 km²), and to analyse the influences of different parameters, such as soil cover, land use, and amount and intensity of rainfall. Other than the above mentioned studies, we used a DEM with a 30 m resolution, a newly compiled map with a soil–topography relationship, and a newly developed land use map served as a spatial basis for modelling discharge. To overcome the problem of incomplete and fragmentary temporal and spatial resolution of available weather data, we used data series from three climatic stations and from Climate Forecast System Reanalysis (CFSR), which were statistically tested with available measured data and excluded if the goodness of fit was unsatisfactory. This enabled a continuous modelling from 1982 to 2010. After new hydropower infrastructure was built, such as the Tana-Beles hydroelectric power plant in 2010, discharge was artificially controlled and could no longer be reasonably modelled.

To consider the different hydro-climatic conditions in the Ethiopian Highlands, the whole upper Blue Nile basin was split into eight sub-basins (>3500 km²). Such a splitting is assumed to help with locating inconsistencies or uncertainties during calibration of the sub-basins and to enable further analysis and follow-up modelling on the sub-basin level. Furthermore, no high computing power is needed for the modelling and calibration of smaller sub-basins, and processes can be distributed to different computers to save time. Discharge was modelled with the Soil and Water Assessment Tool (SWAT) [31], and calibrated and validated with available measured discharge data from the outlets of seven sub-basins using the Sequential Uncertainty Fitting (SUFI-2) programme [32,33]. With the parameters giving the best objective function in the calibration process, discharge was simulated for the entire modelling period at the watershed level, and drainage ratios were calculated with precipitation data from the weather station closest to the centre of every watershed.

The simulations of the drainage ratio with a high spatial and temporal resolution allows detailed analyses of the impact of different parameters (e.g., precipitation, soil type, land use, and slope) on runoff generation. These model possibilities and knowledge gained will further help to assess and improve cultivation strategies in terms of blue and green water use for the long-term planning of local, national, and international water, energy, and food security.

2. Materials and Methods

2.1. Study Area

The upper Blue Nile basin originates in Lake Tana and has its outlet at the border to Sudan. The basin covers a large part of the Ethiopian Highlands (175,000 km²), from an altitude of less than 500 meter above sea level at the Sudanese border to more than 4200 meter above sea level in the centre and the eastern escarpment of the Ethiopian Highlands (see Figure 1). The climate is dominated by the movement of air masses associated with the Inter-Tropical Convergence Zone (ITCZ). During the dry season from November to March, the highlands are affected by a dry north-eastern continental air mass. From March to May, the ITCZ brings a small rainy season (Belg) to the north-eastern part of the basin. Later in the year, the south-western airstream extends over the entire basin and causes the major rainy season (Kremt) from May to October [34]. The Kremt accounts for a large proportion of the mean annual rainfall and this proportion generally increases with altitude [15]. The movement of air masses and the different altitudes are the reason for the different rainfall patterns within the study area. While the northern, western, and southern parts of the study area have one prolonged rainy season from May to September, the eastern part is characterized by a bimodal rainfall regime. To capture these temporal and spatial differences of seasonal climate, the upper Blue Nile basin was split into eight sub-basins of major tributaries with available discharge data, where seven sub-basins were modelled, calibrated, and validated.

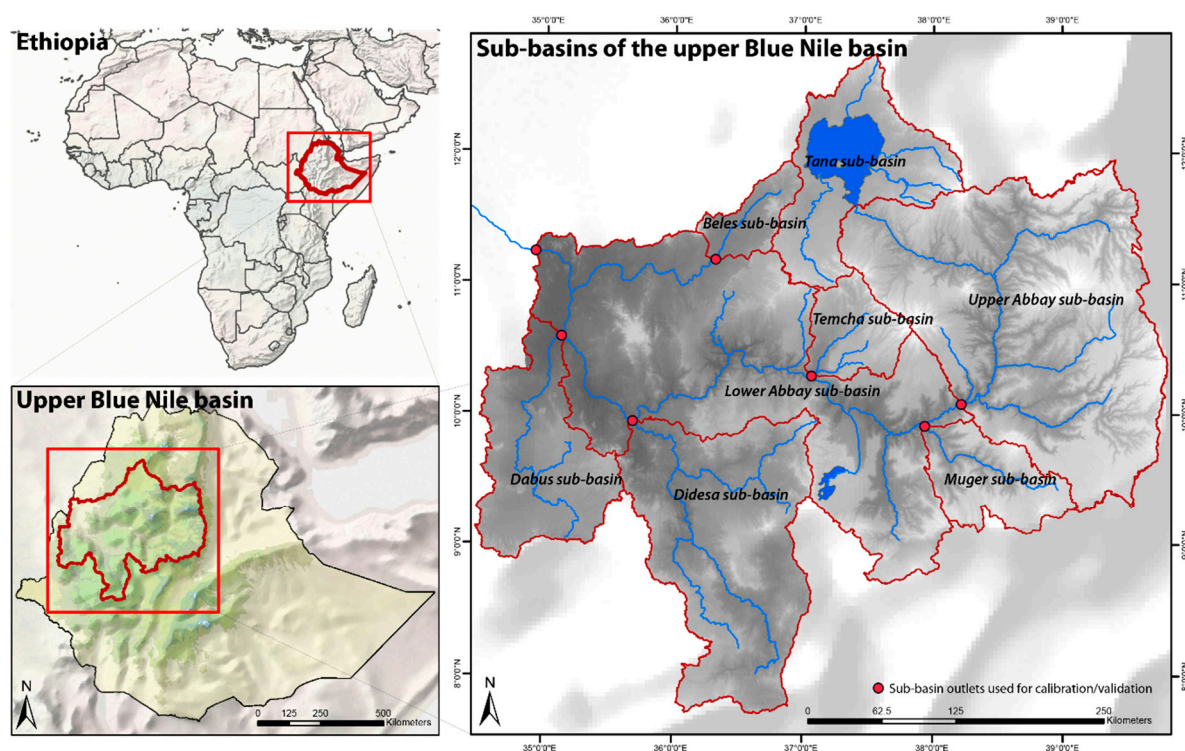


Figure 1. Overview of the upper Blue Nile basin and its sub-basins.

- Lake Tana sub-basin

The source of the Blue Nile, the Lake Tana sub-basin, is dominated by a large shallow lake and its surrounding floodplains. These wetlands and several water resource projects, such as hydropower schemes and dams for irrigation and flood control purposes [35], make modelling difficult, because only little data are available on these natural and human influences. We therefore did not model the Lake Tana sub-basin, but used discharge data from the outflow of Lake Tana from 1982–2010 as inflow to the Upper Abay sub-basin. Since the inauguration of the Tana-Beles hydropower scheme in 2010,

the river regime has changed [36]. However, as no data were available after this change, we were unable to reasonably model more recent runoff.

- Upper Abay sub-basin

The Upper Abay sub-basin is not a tributary, but contains the upstream part of the upper Blue Nile basin between Lake Tana and the Dessie Bridge. Further upstream, no discharge data from the upper Blue Nile River or major tributaries were available. The outlet of Lake Tana was used as inlet discharge for the Upper Abay Sub-basin. The eastern part of the basin is dominated by two rainfall patterns, while the western part has a unimodal rainfall regime. These differences have an impact on plantation activities, and the cropping calendar varies greatly within the sub-basin. For this reason, the cropping calendar of all the watersheds east of the upper Blue Nile and the Beshilo River contains a second crop. In addition to selected CFSR climatic data, we used precipitation data from two observatories of the Water and Land Resource Centre (WLRC) at the eastern borders of the upper Blue Nile basin where data was available for more than 30 years. Average annual precipitation ranges from 500 mm in the northeast to 1750 mm in the northwest.

- Muger sub-basin

More than 75% of the Muger sub-basin is cultivated, mainly with barley and teff. Annual precipitation of only 1200 mm is distributed over two rainy seasons, so we used the cropping calendar from the eastern part of the Blue Nile basin. Recent studies showed that the aquifer system of the Muger sub-basin has a hydraulic connection with the aquifer system of the Upper Awash basin, a basin which does not drain into the Blue Nile [37,38].

- Temcha sub-basin

The Temcha sub-basin is located in the southern Gojam region. More than 70% of the whole sub-basin is cultivated or used for pasture. At 1680 mm, the Temcha sub-basin has the highest average annual precipitation of the whole upper Blue Nile basin. However, the highest measured discharge peaks during the rainy season could still not be simulated with the available precipitation data. Rainfall data originates not only from CFSR, but also from the WLRC observatory at Anjeni [39].

- Didesa sub-basin

The Didesa River originates in the Mt. Vennio and Mt. Wache ranges, and is, together with the Anger River, the largest tributary of the upper Blue Nile basin in terms of the volume of water. In the highlands, long-term mean annual precipitation reaches up to 2000 mm, while the lower area receives on average less than 800 mm precipitation per year.

- Dabus sub-basin

The Dabus sub-basin drains the southwestern part of the Blue Nile basin. In its headwater is an area of wetlands of approximately 900 km² [16]. The whole sub-basin has a size of 14,700 km², over 40% of which is cultivated.

- Beles sub-basin

The Beles sub-basin, located in the western part of the upper Blue Nile basin, abuts the Tana basin and is today linked with the Tana Beles hydropower scheme. With the inauguration of this scheme in 2010, the drainage behaviour of Lake Tana changed and it was no longer possible to model the discharge of the whole upper Blue Nile basin, due to missing data from the outlets of Lake Tana. The size of the sub-basins was reduced to only 3500 km² and delimited by the Upper Main Beles gauging station, because of inconsistent available discharge data from the main outlet of the Beles River. The small sub-basin has on average 1570 mm precipitation per year, and is dominated by shrubland, grassland, and pasture (70%).

- Lower Abay sub-basin

The lower Abay sub-basin contains the area along the upper Blue Nile basin below the Didesa Bridge, which could not be modelled with larger tributaries. The Upper Abay and all the five modelled tributaries flow into this sub-basin and were included as basin inlets.

2.2. Hydrological Model

For this study, we used SWAT to simulate the discharge of the sub-basins in the upper Blue Nile basin. Other modelled physical processes, such as potential evapotranspiration and base flow [40], were calculated with the Hargreaves Method [41] and an automated base flow separation and recession analysis technique [42], respectively, and used to control the plausibility of the shares of these processes. However, due to a lack of measured data, they could not be calibrated and validated. The model requires input parameters, such as soils, land use, land management, topography, or climate data [43]. It is designed to calculate runoff and sediments for individual drainage units, called hydrologic response units (HRUs), in generated sub-catchments. It also routes modelled discharge and sediment load towards the outlet of the basin [44]. A more detailed description of the model can be found in many reviews of its performance and parameterization in Ethiopia and other regions [9,14,45–50].

2.3. Model Input and Setup

2.3.1. Topographical and Land Use Data

For the topographic map this study used the Advanced Spaceborne Thermal Emission and Reflection Radiometer (ASTER) Global Digital Elevation Model Version 2 (GDEM V2) from the Ministry of Economy, Trade, and Industry (METI) of Japan and the United States National Aeronautics and Space Administration (NASA) of a 30 m resolution [51] (see Appendix C).

Regarding land use and land cover (LULC) information, most available data sets were found to be outdated and produced with a spatial resolution insufficient to represent the heterogeneity of the study area, which was the main focus of this study. The data sets in question are the Global Land Cover Characterization (GLCC) database of the United States Geological Survey (USGS) with a spatial resolution of 1 km [17], the map from the Eastern Nile Technical Regional Office (ENTRO) with five dominant LULC categories [10], or the data from BCEOM [52] with seven dominant land cover categories [53,54]. Other high resolution land use maps are only available for small watersheds, such as the land use maps from the Water and Land Resource Centre (WLRC) [55]. Kassawmar et al. [56] produced a land cover dataset for the Ethiopian Highlands with a resolution of 30 m. Due to cloud and haze cover, it was not possible to use images from only one specific year. The applicability of such data sets for a similar purpose was explained in the Economics of Land Degradation (ELD) Ethiopia Case Study [57]. For the present study, we needed additional land use classes that could explain the very heterogeneous land use, management, and practices. The required information was missing in the data set produced by Kassawmar et al. [56]. For that reason, we added new classes, based on the 35 land cover classes used in the ELD Ethiopia Case Study. We identified the new classes by integrating different auxiliary data sets, such as farming, cropping system, and livelihood zone maps of the Food and Agriculture Organization (FAO) [58], agro-ecological zone maps [59], and local knowledge. All the different crops growing in the highlands of Ethiopia could not be distinguished at the pixel level with a 30 m × 30 m pixel resolution. Moreover, due to crop rotation practices, it was not reasonable to assign one land use category to a certain area. For these categories, e.g., BWTF (barley, wheat, and teff), the most prevalent crop types were selected and for the different crop parameters in SWAT, the average value of the three crop types was used (Figure 2 Appendix B).

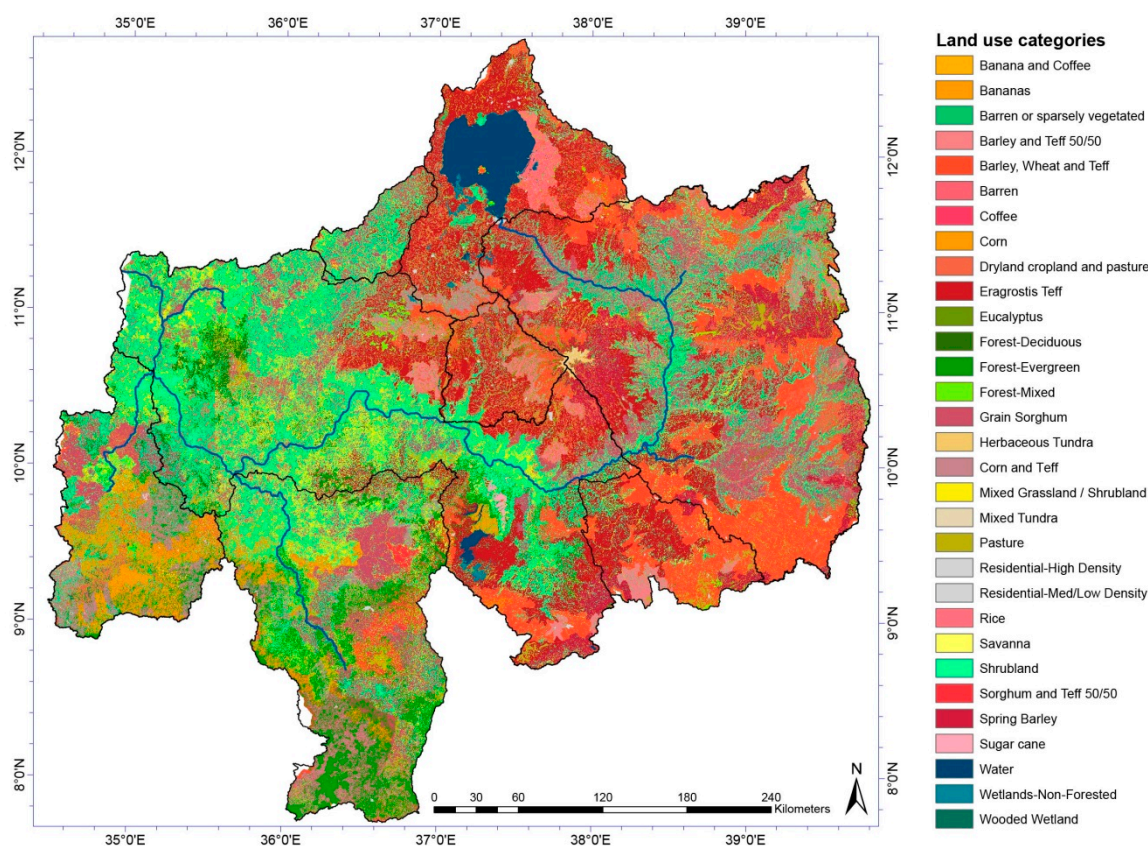


Figure 2. Newly developed land use map.

More than 20% of the whole upper Blue Nile basin is categorized as shrub/bushland (SHRB). This is because especially along the gorges and in the western part of the basin, towards the outlet, many areas are covered in different kinds of shrubs. Teff is the staple crop of Ethiopia and covers more than 13% of the study area (see Appendix D). It grows at a wider altitude range and exists in combination with other crops. Thus, the land use is characterized by a combination of teff with other land use categories, which include more than one crop type; BWTF (barley, wheat, and teff), COTF (corn and teff), BATF (barley and teff), and SGTF (sorghum and teff). The planting dates of the different crops were adapted according to the rainfall pattern. In the eastern part, where two rainy seasons allow the farmers to plant two crops on the same field in one year, the cropping calendar of Loetscher [60] was used. For the other part of the basin, with only one prolonged rainy season, the planting dates were adapted to the cropping calendar by Ludi [61]. The growing duration of the different crop types was scheduled by pre-defined heat units and the auto-fertilization and auto-irrigation option of SWAT were used to simulate crop growth. Tillage was adapted to the use of the traditional Ethiopian *maresha* plough with a random roughness (RRNS) of 25 mm, a depth of mixing (DEPTIL) of 150 mm, and a mixing efficiency of 0.3 (EFTMIX) [62,63].

2.3.2. Soil Data

The most detailed available soil information in Ethiopia at the basin level are from the Harmonized World Soil Database (HWSD) [64]. However, because these soil data are not related to topography, Brunner [65] generated a soil map for Ethiopia with a soil-topography relationship, but with only the superordinate soil categories (see Appendix A).

To obtain a soil map with the soil-topography relationship from Brunner [65] and the specific soil categories of HWSD, we reclassified the map of Brunner with the soil categories of HWSD (see Figure 3). For the reclassification, we considered the spatial and geomorphological appearance of the

different soil types. The 19 soil types (+water) of the new soil map of the upper Blue Nile basin were linked with the soil parameters of the SWAT database to run the model and to simulate discharge.

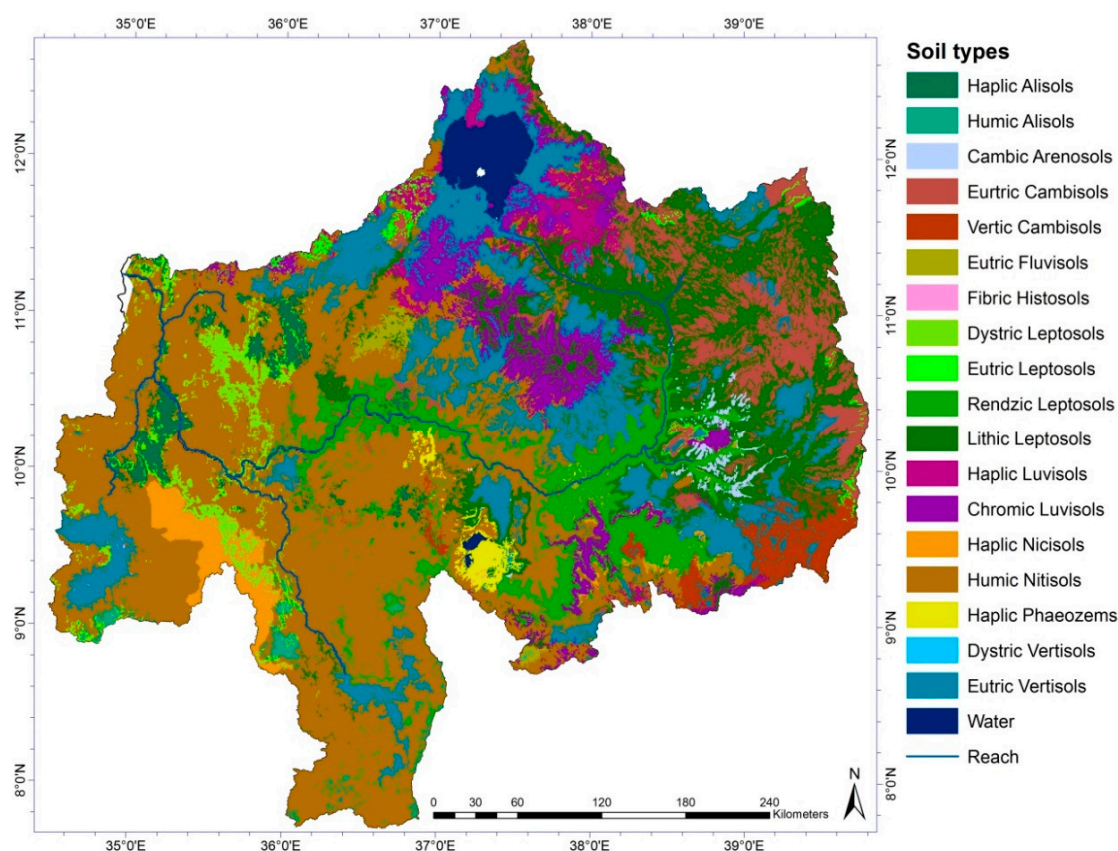


Figure 3. Newly generated soil map.

2.3.3. Climate and Hydrological Data

The density of available measured discharge and temperature data in the Ethiopian Highlands is low: Most of the time series are error-prone and have a lot of missing data. Therefore, the only available measured complete data set from three observatories from the Water and Land Resources Information System [39] have been complemented with generated data from the National Centers for Environmental Prediction (NCEP). This Climate Forecast System Reanalysis (CFSR) precipitation and climate data (minimum and maximum temperature, solar radiation, wind speed) are available from the Texas A&M University (TAMU) spatial science website (www.globalweather.tamu.edu, accessed May 2017) for the entire upper Blue Nile basin (bounding box: Latitude 8.60–12.27 N and longitude 33.94–40.40 E). Previous studies showed that these data are unsuitable for small-scale catchments in the upper Blue Nile basin [66], but according to Dile and Srinivasan [62], CFSR weather is a viable option for hydrologic modelling in data-scarce regions on a larger scale, like the Ethiopian Highlands. For this reason, we compared CFSR rainfall data with available, but incomplete, precipitation data from 35 meteorological stations of the National Meteorological Agency of Ethiopia (NMA) with a statistical goodness of fit of time series (NSE, R^2 , mean error, PBIAS) and excluded unrealistic CFSR weather points. Finally, 43 CFSR climate and precipitation point stations were used as well as three local weather stations from WLRC to simulate the discharge of the whole upper Blue Nile basin and to calculate the drainage ratio for the delineated watersheds. Potential evapotranspiration was simulated with the Hargreaves method [41]. For discharge calibration, we used measured data from the NMA for the outlets of eight sub-basins. Due to the incomplete time series, the calibration and validation period of the sub-basins contain different years (see Table 1).

Table 1. Information on the sub-basins.

Characteristics of the Sub-Basins for Modelling	Lake Tana	Upper Abay	Muger	Dabus	Didesa	Temcha	Beles	Lower Abay
Name of gauging stations *	Outlet Bahir Dar	Kessie	Outlet Muger	Outlet Dabus	Outlet Didesa	Outlet South Gojam	Beles Headflow	Border Ethiopia-Sudan
Area of hydrological catchment (km ²)	15,700	48,800	7300	14,700	28,200	5500	3500	51,000
Watersheds/HRUs	Not modelled	64/13,336	41/8198	15/2521	54/8670	23/4245	10/1638	116/22,026
Altitude range (m a.s.l.)	1696–4102	1011–4245	965–3522	467–3130	609–3210	784–4088	944–2736	446–3948
Available discharge data (year)	1982–2010	1983–2004	1982–1992	1982–1992	1982–1992	1986–2010	1984–2002	1982–2010
Calibration period (year)	Not modelled	1996–2004	1987–1992	1987–1992	1987–1992	1987–1992	1995–2002	1988–1995
Validation period (year)	Not modelled	1988–1995	1982–1986	1983–1986	1982–1986	1982–1986	1989–1994	1996–2004

* According to the National Meteorological Agency of Ethiopia (NMA).

2.3.4. Modelling Approach

- The upper Blue Nile basin was divided into eight sub-basins where sufficient discharge data were available (see Figure 1). Seven sub-basins were simulated individually with SWAT [31,40] and also individually calibrated and validated with the SUFI-2 programme [32,33,67]. The topmost sub-basin with the outlet of Lake Tana was not modelled, due to human activities for which no data were available, such as irrigation and damming up the lake. Instead of simulated data, we used available discharge data from the outlet of Lake Tana (1985–2010) from the NMA as an inlet of the subsequent Upper Abay sub-basin. Other water infrastructure was not incorporated into the model, because there was no data available or the influence on the total discharge was negligible;
- with the parameters giving the best objective function in the calibration process, discharge was simulated for the whole time period (1982–2010) of the sub-basins starting with the upstream sub-basins;
- the newly simulated discharge of each sub-basin was used as the inlet discharge for the next lower sub-basin;
- the total discharge of the upper Blue Nile basin was finally calibrated and validated at the outlet of the Lower Abay sub-basin, which is the border of Sudan and today the outlet of the Grand Ethiopian Renaissance Dam; and
- with this complete discharge data set comprising modelled data for all delineated watersheds, the percentage of precipitation leaving the watersheds through the river (drainage ratio) could be calculated on a monthly resolution with precipitation data from the next available weather station.

In total, the whole modelled upper Blue Nile basin was divided into seven sub-basins, 323 watersheds, and 60,634 hydrological response units (HRU). In SWAT, the delineated watersheds are defined as sub-basins of the defined sub-basins of the upper Blue Nile basin. For every sub-basin, a three-year warm-up period was selected, which allowed the model to initialize and stabilize starting values for the modelled parameters [55].

2.3.5. Sensitivity Analysis and Calibration Setup

The calibration and validation period was chosen based on the discharge data available for the different sub-basins (Table 1). For all sub-basins, 13 sensitive discharge parameters were chosen according to the literature [66,68–70]. After an individual sensitivity analysis with the same parameter ranges for all sub-basins, insensitive parameters were excluded for the final calibration and validation process (see Appendix F). Finally, three to five calibration iterations (500 simulations each) were carried out for every sub-basin [33].

The goodness-of-fit of the calibration and validation was quantified with hydrographic observations and five model evaluation statistics, such as the widely used coefficient of determination (R^2) and Nash-Sutcliffe efficiency (NSE) [23,71,72], the P-factor and R-factor, and the objective function, bR^2 . The P-factor is the percentage of observed values inside the 95% prediction uncertainty band (95PPU) and ranges between 0 and 1. The R-factor is the thickness of the average 95PPU band divided

by the standard deviation of the observed data. A P-factor of 1 and R-factor of 0 is a simulation that exactly corresponds to the measured data [67]. The percentage of measurement error in SUFI-2 was set to 0. In order to compare the measured and simulated discharge, this study used bR^2 as an objective function [33], which is a slightly modified version of the efficiency criterion defined by Krause et al. [73]:

$$bR^2 = \begin{cases} |b|R^2 & \text{if } |b| \leq 1 \\ |b|^{-1}R^2 & \text{if } |b| > 1 \end{cases} \quad (1)$$

where b is the slope of the regression line between the observed and simulated runoff and R^2 is the coefficient of determination to represent the discharge dynamics. The minimum value of the objective function threshold was set to 0.6; according to Faramarzi et al. [74] and Schuol, Abbaspour, Yang, et al. [75], bR^2 should be ≥ 0.6 to be sufficient.

So far no absolute criteria for judging model performance have been firmly established in the literature [43]. Acceptable statistical measures are always project specific [76]. However, Moriasi et al. [71] and Andersen et al. [77] have proposed to judge a calibration and validation result as “very good” if $NSE > 0.75$ and $R^2 > 0.95$, “good” if $0.65 < NSE \leq 0.75$ and $0.85 < R^2 \leq 0.95$, and “satisfactory” if $NSE > 0.5$ and $R^2 > 0.7$. Satisfactory P- and R-factors depend on the quality of the measured data. If the measured data are of high quality, then the P-factor should be > 0.8 and R-factor < 1 [33]. However, according to Schuol et al. [75], a P-factor > 0.5 and R-factor < 1.3 are still sufficient under less stringent model quality requirements.

3. Results and Discussion

3.1. Calibration-Uncertainty Analysis

Discharge was calibrated for seven sub-basins within the upper Blue Nile basin. Different periods were selected according to the measured data available. Sensitivity analysis with SUFI-2 was carried out by keeping the chosen parameters constant, while varying one parameter in a realistic range [33]. The sensitivity of the parameter varied in the different sub-basins, but the most sensitive were GW_DELAY (groundwater delay), RCHRG_DP (deep aquifer percolation fraction), and CN2 (runoff curve number). For calibration and validation, we selected 11 to 13 parameters for their individual sensitivity (see Appendix F).

Calibration and validation were first conducted in the sub-basins with no inlet from other sub-basins, except for the Upper Abay sub-basin, where the outlet from Lake Tana (in Bahir Dar) was used as the inlet. Due to different available discharge data, the length of time varied in the different sub-basins for calibration and validation (see Figure 4).

The overall goodness-of-fit for the different discharge calibration and validation varies from “satisfactory” to “very good”, except for the Muger and Dabus sub-basins, where the NSE is slightly unsatisfactory for the validation period (see Table 2). In the Muger sub-basin, this results from a very low measured base flow during the dry season, which could not be simulated properly. An explanation for this discrepancy is the aquifer system of the Muger sub-basin, which has a connection with the aquifer system of the Upper Awash basin [37,38]. These water losses were not included in the model setup. In the Dabus basin, a discharge shift is the cause of unsatisfactory modelling results. One reason is the presence of wetlands in the Dabus headwater [16], where water can be stored and lead to delayed discharge, which was not modelled properly. Like the Muger sub-basin, the Temcha sub-basin also shows an unsatisfactory P-factor: This is the result of very high measured discharge peaks during the rainy season, which could not be simulated with available precipitation data. In the Lower Abay sub-basin, the low P-factor and R-factor can be explained by the high share of the streamflow coming from the upstream sub-basins; only roughly 25% of the streamflow is generated within the catchment. Therefore, realistic parameter ranges have only a small impact on total discharge and the thickness

of the average 95PPU band does not become wide enough to cover a higher percentage of measured discharge. However, the overall goodness-of-fit for the final outlet of the upper Blue Nile basin can be judged as “satisfactory”—and for the calibration period, when most upstream sub-basins have been calibrated, even as “good” to “very good”.

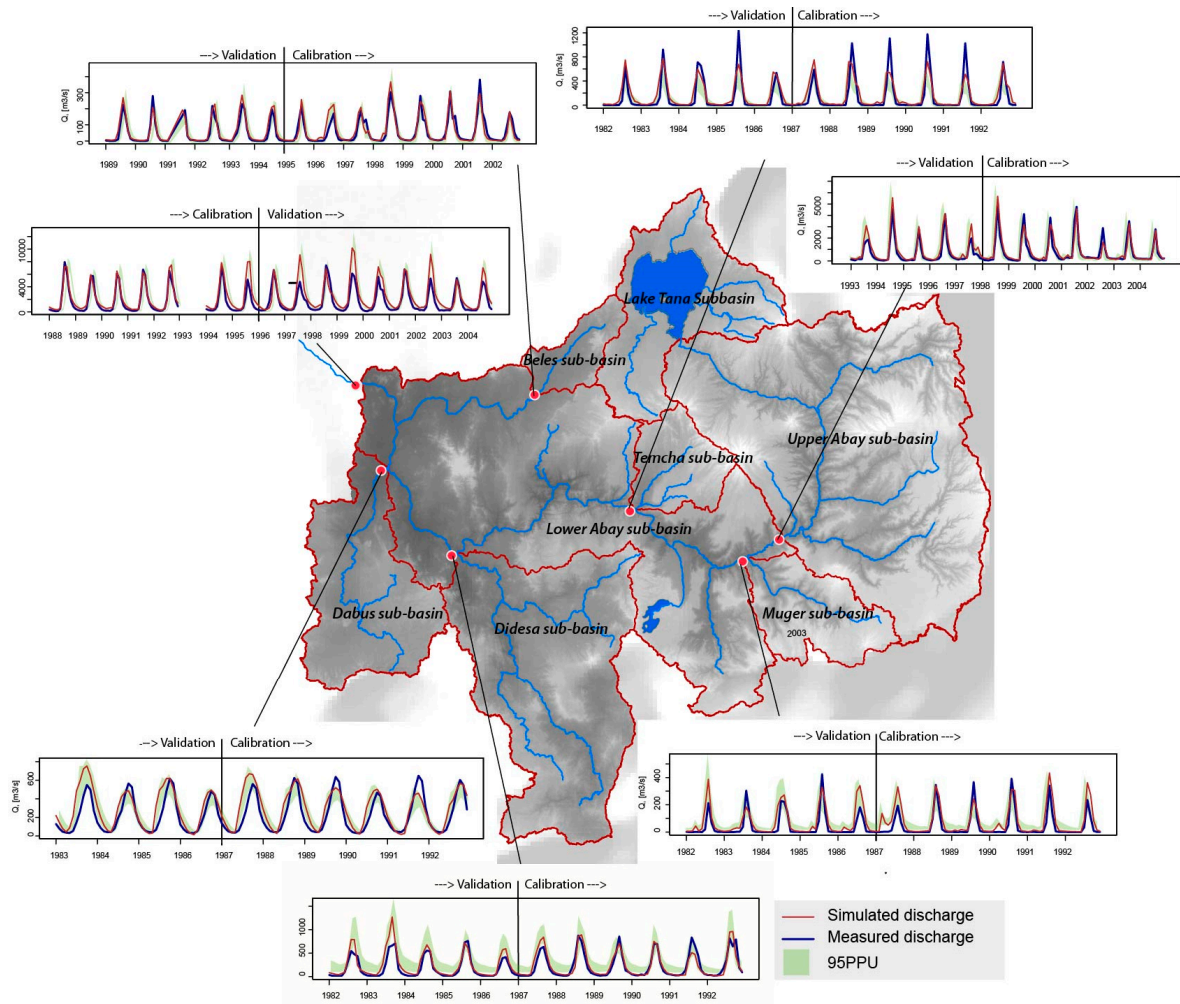


Figure 4. Hydrographic model calibration and validation results: Observed discharge and discharge simulated with the parameters giving the best objective function in the calibration process at the seven outlets of the sub-basins.

Table 2. Final calibration and validation statistics for the seven sub-basins in the upper Blue Nile basin.

Sub-Basin	P-Factor		R-Factor		R ²		NSE		bR ²	
	Cal	Val	Cal	Val	Cal	Val	Cal	Val	Cal	Val
Upper Abay	0.62	0.43	0.77	1.01	0.87	0.95	0.87	0.79	0.84	0.74
Muger	0.18	0.17	0.88	1.03	0.80	0.69	0.60	0.44	0.68	0.61
Temcha	0.24	0.18	0.44	0.52	0.78	0.78	0.76	0.76	0.67	0.67
Didesa	0.58	0.40	1.03	1.35	0.84	0.84	0.82	0.64	0.83	0.68
Dabus	0.64	0.65	0.75	0.92	0.76	0.75	0.66	0.45	0.70	0.61
Beles	0.78	0.83	0.67	0.69	0.85	0.90	0.83	0.86	0.84	0.83
Lower Abay	0.24	0.17	0.42	0.50	0.89	0.80	0.82	0.51	0.80	0.62

Note: Cal = calibration, Val = Validation.

3.2. Modelling Approach Discussion

Unlike previous studies (see introduction), this study did not model the whole upper Blue Nile basin in one run. The upper Blue Nile basin was divided into seven sub-basins, each of which was modelled separately. Due to incomplete time series and gaps in the measured data, the measured outflow was only used for calibration and validation, and a complete time series of the modelled outflow was used as an inlet for the subsequent sub-basin. Sensitivity analysis of the calibrated parameters was very different for each sub-basin, and the final parameter ranges also differed for every sub-basin (see Appendix F). This indicates that every sub-basin has its own characteristics due to differences in e.g., topography, land management practices, or rainfall patterns. If using only one model for the whole upper Blue Nile basin, it is difficult to locate inconsistencies or uncertainties during calibration at the basin or watershed level. In addition, the data on the seven sub-basins can be used for further analysis, and follow-up modelling (in sediment, land use/land cover change, or climate change) can be conducted on the sub-basin level.

A further advantage of the divided basin is of a technical nature: When modelling the whole upper Blue Nile basin using the given spatial resolution, high computing power is required for modelling and calibration. By splitting up the upper Blue Nile basins into different sub-basins, modelling, calibration, and validation can be carried out on a usual desktop computer, and the processes can be distributed to different computers to save time. This issue is crucial if the model is being used by different research teams.

3.3. Spatial Variabilities in Drainage Ratio

The highest average annual drainage ratios can occur in the southwestern, northern, and eastern part of the upper Blue Nile basin (>0.6). Low drainage ratios can be observed along the valley of the upper Blue Nile River, in the Didesa sub-basin, and in the north-eastern part of the upper Blue Nile basin (less than <0.1) (see Figure 5 and Figure S1). These spatial variations in drainage ratio are the results of different rainfall patterns and amounts of annual rainfall (compare Figure 5, Figure 6 and Figure S1). The most important observation is that drainage ratios increase with higher amounts of precipitation. The correlation ($r = 0.54$) is shown in Figure 6 (left), with the mean annual precipitation and drainage ratio data from the 323 watersheds in the upper Blue Nile basin. This correlation was already observed by Lemann et al. [30] in a comparison of the different hydrological responses of three small-scale catchments in the upper Blue Nile basin; after a predefined amount of precipitation, additional rainfall apparently increases the share of blue water leaving a catchment. Liu et al. [78] and Steenhuis et al. [79] discussed an effective precipitation threshold (precipitation minus potential evaporation) of 500 mm, where hydrological response can be predicted by its linear relationship to precipitation. Sub-basins with high amounts of rainfall have a higher drainage ratio and therefore a disproportional increase in blue water, compared to dryer sub-basins.

Nevertheless, the drainage behaviour of every sub-basin is different, not only because of different precipitation rates, but also because of different characteristics and individual calibration. For example, the Didesa sub-basin has an average drainage ratio of 0.21, while in Dabus, the average drainage ratio is as high as 0.52 (see Table 3), with almost the same long-term mean annual precipitation (1424 mm and 1418 mm). One reason for these differences can be found in the slope and different land use cover of the two sub-basins: The Dabus sub-basin has an average slope of 14% and land use is dominated by cultivated areas ($>40\%$) and shrubland (20%), while Didesa has an average slope of 12% and the most common land use types are forest and shrubland (22% and 19%). This is also one explanation for the differences between the Temcha and the Beles sub-basins, which have almost the same annual precipitation, but different average drainage ratios (0.55 and 0.37).

Table 3. Rainfall distribution and modelling results of drainage ratios for the seven sub-basins.

Rainfall Characteristics of the Sub-Basins	Upper Abay	Muger	Dabus	Didesa	Temcha	Beles	Lower Abay
Rainfall pattern	Unimodal/Bimodal	Bimodal	Unimodal	Unimodal	Unimodal	Unimodal	Unimodal
Av. annual precipitation (1985–2010) (mm)	1140	1200	1420	1420	1680	1630	1570 *
Av. annual drainage Ratio (1985–2010)	0.37	0.28	0.52	0.21	0.55	0.37	0.25

* 1988–2010.

The Temcha watershed is intensively cultivated (>70% crop and pasture), while shrub and grassland (>50%) dominate in the small Beles watershed. Other studies support the modelling results: e.g., Hurni et al. [80] found at the plot level, 5–40 times more runoff from degraded and cultivated lands than from forest lands. A higher share of forest means among other parameter changes, a lower curve number and higher leaf area index, both of which result in lower surface runoff [81,82] and a higher evapotranspiration rate. Higher evapotranspiration rates, e.g., in the Didesa and Beles sub-basins, were also shown by Allam et al. [18].

Land use change dynamics, with an increase in farmland and settlement and a decrease in forest and shrubland, will therefore lead to a higher share of blue water, but a lower level of green water in soil and vegetation. Various studies reported a change in land use and land cover where cultivated areas have increased within the last 40 years [24,29,83,84]. Land use/land cover changes could not be shown within this study, as no older land use maps with a comparable resolution were available. Nevertheless, this study shows that an expansion in cultivated area increases surface runoff and thus also the drainage ratio. This effect can be partly reduced with integrated watershed conservation measures, which are also important to reduce sediment yield generation [81].

Another reason for the different shares of blue and green water availability can be found in the different dominating soil types. In the north-western part of the Lower Abay sub-basin, where 24 watersheds receive the same temporal distribution and amount of precipitation, drainage ratios range from 0.44 to 0.56. While the share of forest/shrub and cropland is similar in most watersheds, different soil types can be observed there. Watersheds with high drainage ratios are dominated by Leptosols, and watersheds with a lower share of discharge are covered by Alisols and Nitisols. In the model, the very shallow Leptosols have a defined soil depth of only 25 cm, while Alisols and Nitisols have 1 m and more. Even if Leptosols are moist (to arid), they are only wet for short periods [85] and store less precipitation than Alisols and Nitisols. This results in a higher share of blue water and a higher drainage ratio.

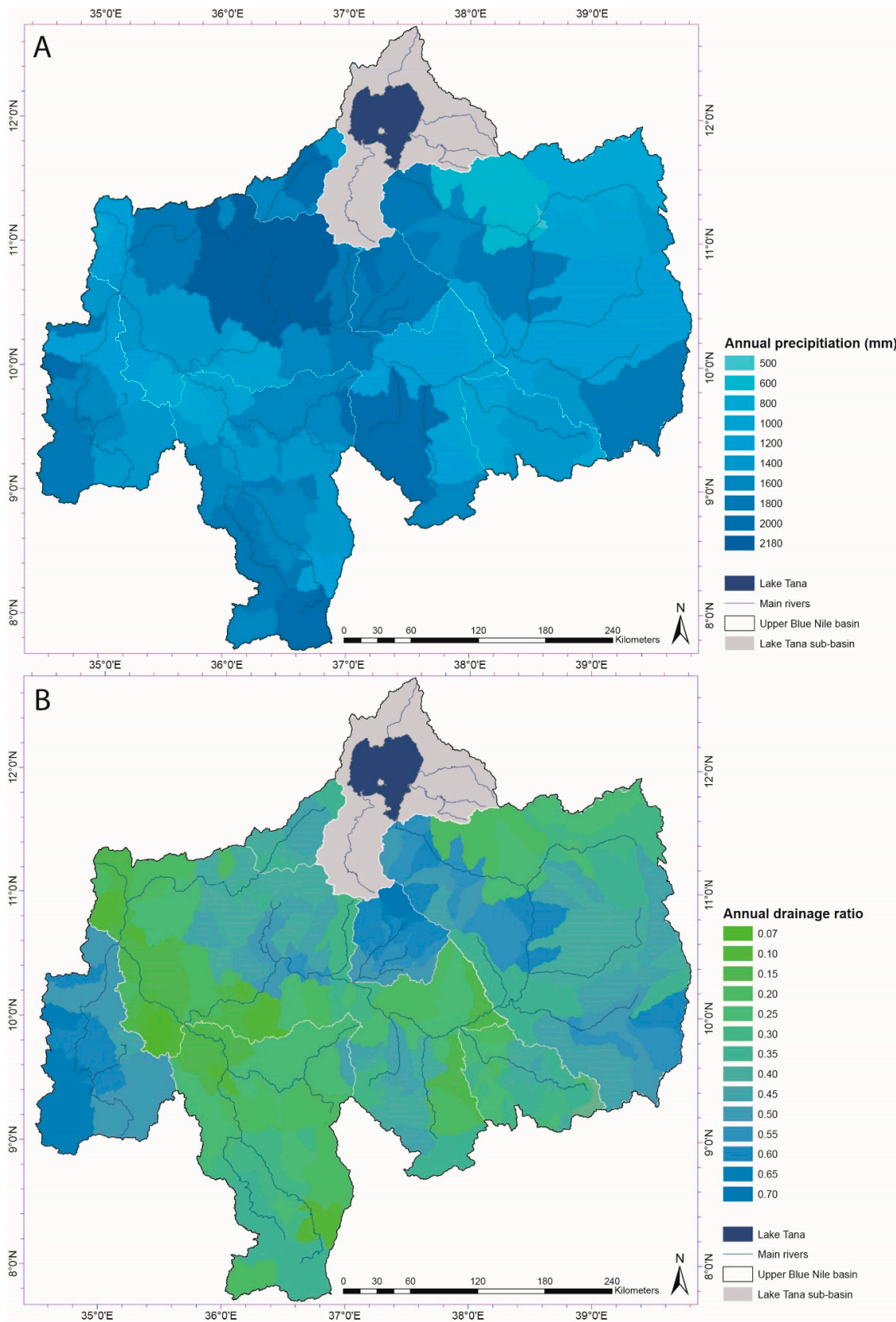


Figure 5. Long-term mean annual drainage ratio and precipitation at the watershed level. Drainage ratios have not been modelled for the Lake Tana sub-basin.

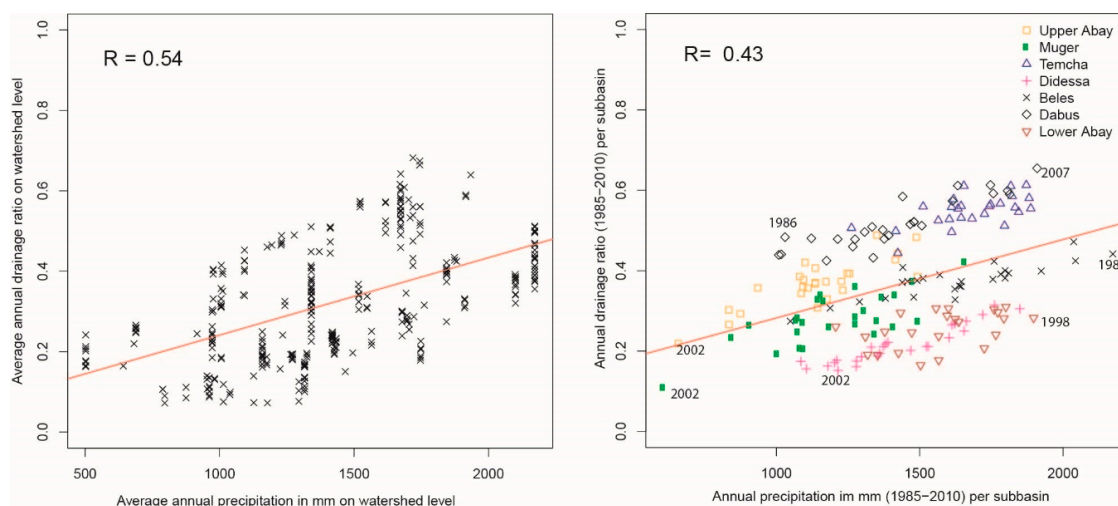


Figure 6. Correlation of drainage ratio and rainfall with a regression line for all data. Left: Mean annual correlation for all 323 watersheds. Right: Annual correlation for every year from 1985 to 2010 for all seven sub-basins.

3.4. Temporal Differences in Drainage Ratio

Drainage ratios of the single sub-basins vary not only within—but also between—years. Figure 6 shows that years with higher precipitation rates generate a higher drainage ratio than dry years, when significantly less water leaves the sub-basins throughout the river. However, rainfall properties, such as duration, intensity, and inter-event duration, also vary in the upper Blue Nile basin [86] and influence the drainage behaviours in dry and wet years differently in every sub-basin. High annual precipitation rates do not necessarily lead to high drainage ratios if rainfall is distributed over several months. In the upper Abay sub-basin, for example, the highest amount of annual rainfall was calculated for 1986 (1493 mm). However, because rainfall was distributed over several months and only 49% of annual rainfall occurred in July and August, less than 40% of rainfall left the sub-basin through the river. This was not the case in 1994, when the drainage ratio reached 0.49: 70% of the annual precipitation occurred in July and August, the two months with the highest share of rainfall (Figure 7 Appendix E) and when, accordingly, most discharge is generated. The lowest drainage ratio (0.22) was calculated in 2002, when the lowest amount of annual precipitation—658 mm—was measured. In 2008 and 2009, annual precipitation was almost the same (835 mm and 834 mm), but the drainage ratio was 0.27 and 0.30, respectively. These differences can again be explained by the distribution and intensity of annual rainfall. In 2009, 77% of the annual precipitation occurred during July (48%) and August (29%), while in 2008, these two months only received a total of 59% (33% in July and 26% in August) and the annual precipitation was distributed more equally over the whole rainy season. These correlations between intensity and temporal distribution of precipitation and drainage ratios can also be observed in the other sub-basins (see Appendix D). Monthly drainage ratios can only be considered in months with a certain amount of rainfall. In a dry month, when discharge is baseflow-dominated, high drainage ratios are not relevant for the total annual drainage ratio, as discharge in these months is very low.

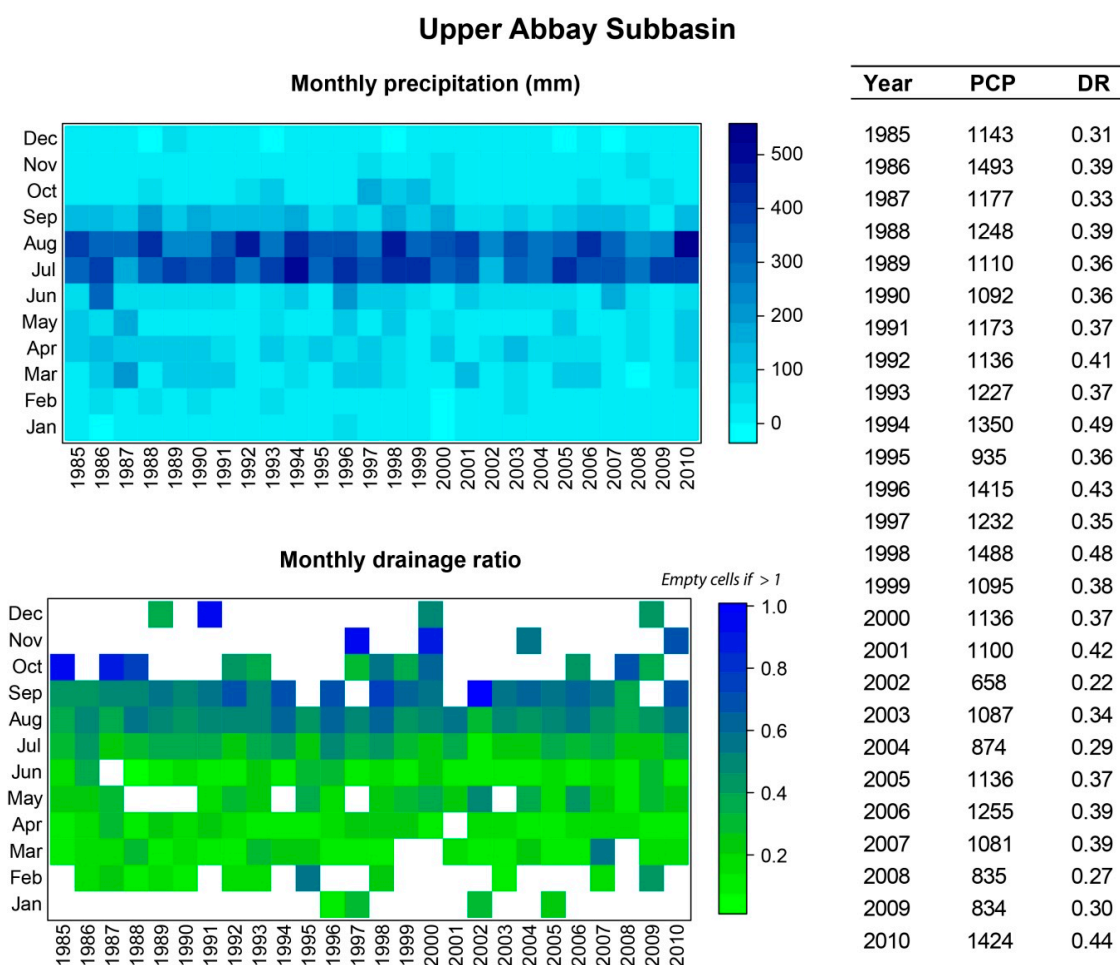


Figure 7. Monthly and annual distribution of precipitation (PCP) and drainage ratios (DR) for the Upper Abay sub-basin. Data for the other six sub-basins can be found in Appendix D.

Most climate change scenario models predict more annual rainfall for the near future; however, variations between models are high [87], as are seasonal variations [88–91]. Higher precipitation would lead to a higher drainage ratio, meaning that the amount of blue water leaving the Ethiopian Highlands would increase disproportionately to precipitation. However, in all cited literature, the scenario models also projected an increase in the annual mean temperature, and as a result, a part of the blue water would convert to evapotranspiration and decrease the drainage ratio and the water for downstream stakeholders [30]. The mutual interaction of precipitation and temperature, and the influence on discharge, are highly dependent on the magnitude of local changes. With the available time series, the effect of changing temperatures could not be shown in this study as there were no significant changes in the amplitude of temperature during the model period. However, using the prepared model as well as the newly available maps and data sets as a basis, further analysis can be performed and different climate scenarios can be modelled at the catchment level.

4. Conclusions

The present study simulated and calculated the long-term drainage ratios of the upper Blue Nile basin in the Ethiopian Highlands. To represent the heterogeneity of the study area, we developed a new soil and land use map to model seven sub-basins of the upper Blue Nile basin with a 30 m digital elevation model, or DEM. With the best parameter range from the calibration and validation process, discharge was modelled for years and areas where no data was available. This allowed us to calculate

and analyse temporal and spatial drainage ratios of 343 watersheds in the upper Blue Nile basin for 26 years (1985–2010).

Our results indicate that in the upper Blue Nile basin, precipitation and drainage ratios vary greatly over the basin and over time. In regions with high annual precipitation levels, drainage ratios are much higher than in dryer areas. In years in which annual precipitation is distributed over the whole rainy season, the percentage of rainfall leaving the watersheds through the river is lower than in years in which most annual precipitation is concentrated over a period of two months. Higher drainage ratios due to different amounts and intensity of rainfall can be explained through higher surface runoff, which is, *inter alia*, the result of saturation-excess processes. Other influencing parameters are the land use, where cultivated land generated a higher share of runoff than a forest-dominated watershed due to less surface runoff and higher evapotranspiration rates. However, soil type is also crucial: Deep Alisols or Nitisols generate lower drainage ratios than, for example, shallow Leptosols.

Looking at different forecasts up to the year, 2100, for changes in climate and land use (the latter due to population growth), we found that several changing parameters cause higher runoff. Areas with a greater level of cultivation and rainfall will have higher drainage ratios and higher amounts of blue water for downstream stakeholders. Only a predicted rise in temperature may partly cushion these effects, due to higher evapotranspiration rates. Nevertheless, the higher amount of available blue water is linked with increasing surface runoff and erosivity. Therefore, the predicted changes in land use and climate are likely to lead to higher erosion rates in the upstream area and increasing sediment loads in the Blue Nile. This is not only a threat to the upstream, mainly rainfed area, where fertile topsoil is being eroded, but also for downstream stakeholders, where high sediment rates are reducing the lifespan of water infrastructure. Only sustainable and integrated watershed conservation measures in areas with high rainfall can cushion these climate and land use change dynamics and reduce soil erosion and sediment loads in the river. Even if such conservation measures can somewhat reduce the drainage ratio over time (by resulting in deeper soil, reduced slopes, changed land use), downstream stakeholders will not receive less water, due to predicted changes in the amount of rainfall and calculated shares of available blue water.

This study contributes to the understanding of hydrological processes and availability of blue and green water in the upper Blue Nile basin. This knowledge is crucial for analysing future changes and improving sustainable and integrated watershed management from which up- and downstream stakeholders will benefit.

Supplementary Materials: The following are available online at <http://www.mdpi.com/2073-4441/11/1/21/s1>, Figure S1 (KMZ): Long-term mean annual drainage ratio at watershed level.

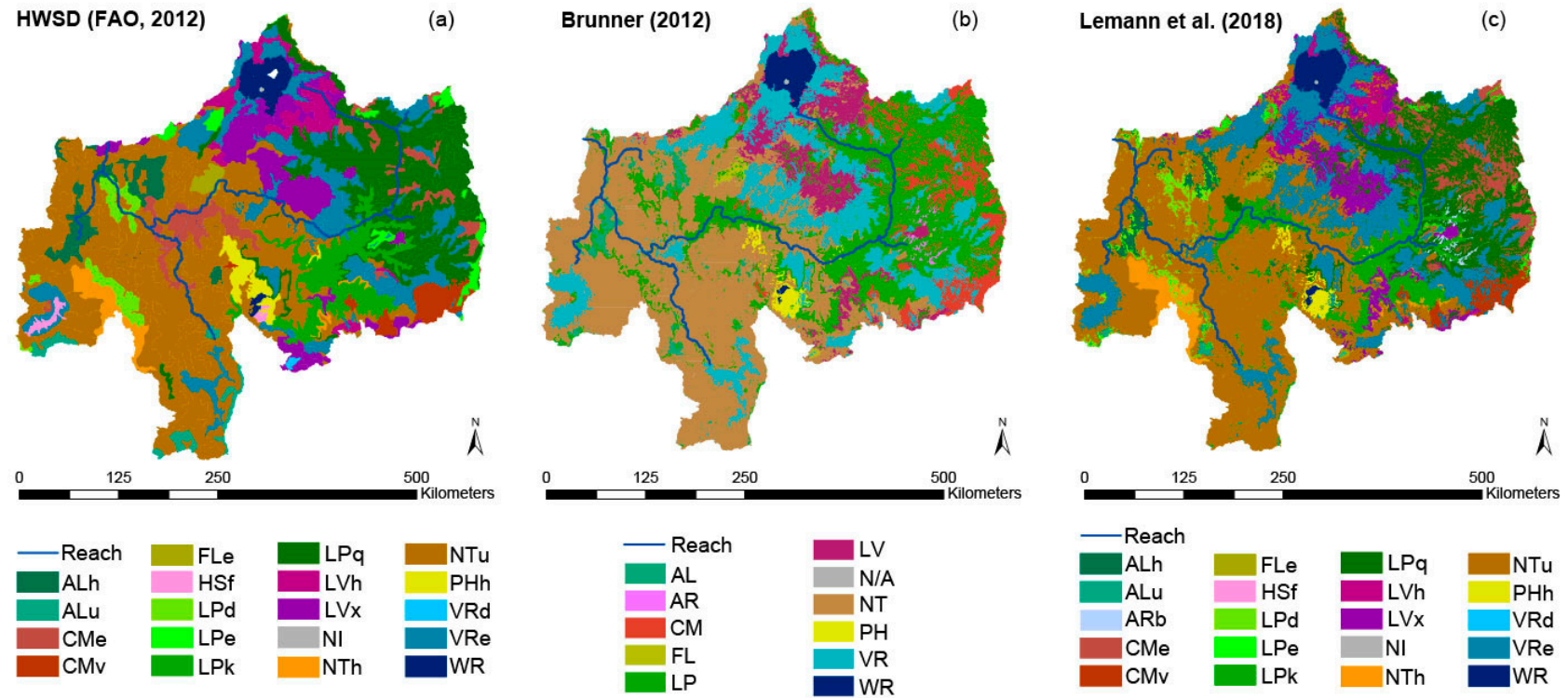
Author Contributions: Conceptualization, T.L.; Data curation, T.L., V.R., G.Z., T.K. and H.H.; Formal analysis, T.L. and V.R.; Investigation, T.L., V.R. and T.K.; Methodology, T.L. and V.R.; Project administration, T.L.; Resources, T.L., V.R., G.Z., T.K. and H.H.; Software, T.L., V.R. and T.K.; Supervision, G.Z. and H.H.; Validation, T.L., V.R., G.Z., A.S., T.K. and H.H.; Visualization, T.L. and V.R.; Writing—original draft, T.L., V.R., A.S., T.K. and H.H.

Funding: This work was supported by the Centre for Development and Environment (CDE) and the Institute of Geography of the University of Bern, Switzerland.

Acknowledgments: We are grateful to the Water and Land Resource Centre, Addis Abeba, Ethiopia, for providing data, and to Tina Hirschbuehl for editing.

Conflicts of Interest: The authors declare no conflict of interest.

Appendix A. Soil Maps in the Upper Blue Nile Basin



Newly generated soil map (c) with the used soil types in the upper Blue Nile Basin (Table) and the two soil maps from the Harmonized World Soil Database without a soil-topography relationship (a) and Brunner (2012) (b) with only the superordinate soil cat.

Used soil classes in the upper Blue Nile basin.

SWAT Soil Type	Soil Types	Upper Blue Nile Basin	
		Area (km ²)	% of Total Area
NTu	Humic Nitisols	61,578.61	35.99
VRe	Eutric Vertisols	24,751.42	14.46
LPq	Lithic Leptosols	24,496.40	14.32
LPk	Rendzic Leptosols	13,344.74	7.80
CMe	Eurtric Cambisols	12,797.05	7.48
LVx	Chromic Luvisols	9544.14	5.58
LPd	Dystric Leptosols	4516.97	2.64
ALh	Haplic Alisols	3790.68	2.22
CMv	Vertic Cambisols	3739.54	2.19
LVh	Haplic Luvisols	3670.93	2.15
NTh	Haplic Nicisols	3370.57	1.97
PHh	Haplic Phaeozems	1324.08	0.77
FLe	Eutric Fluvisols	1115.07	0.65
ALu	Humic Alisols	1092.26	0.64
LPe	Eutric Leptosols	1055.31	0.62
ARb	Cambic Arenosols	900.54	0.53
HSf	Fibric Histosols	24.66	0.01
VRd	Dystric Vertisols	9.26	0.01
TOTAL *		171,122.23	100

* Without water areas.

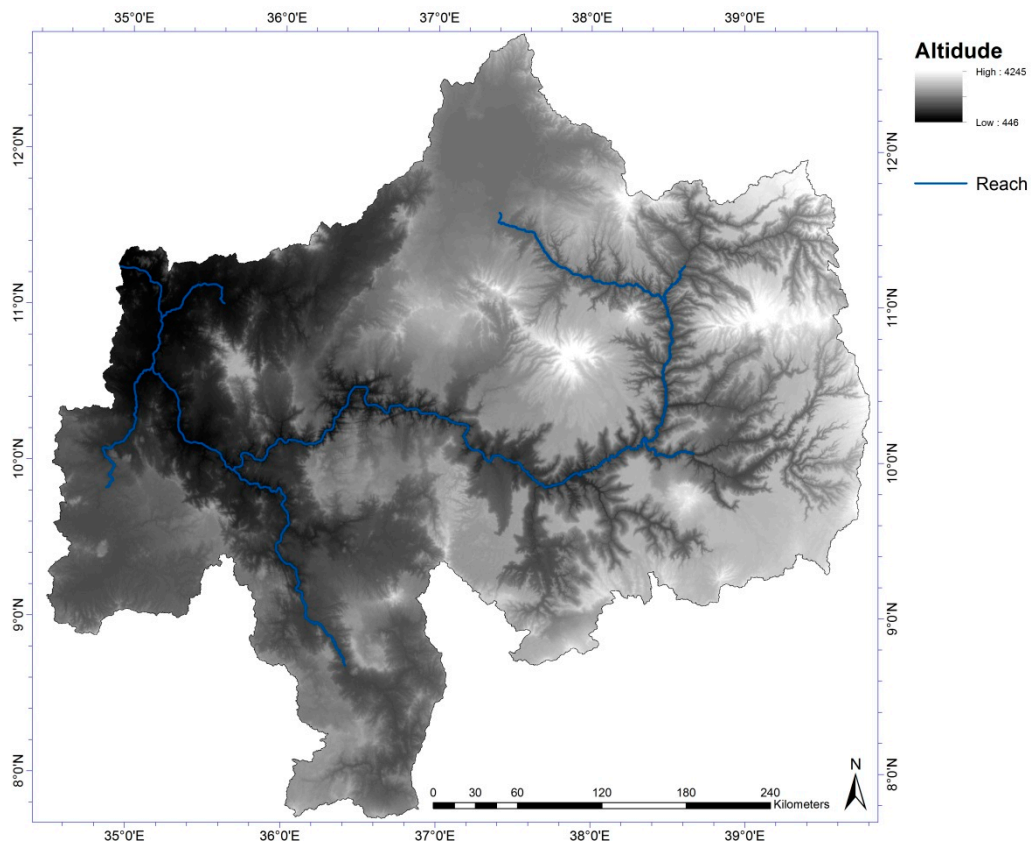
Appendix B

Land use classes in the upper Blue Nile basin (map see Figure 2).

SWAT Land Use Type	Land Use Classes	Crop Rotation (OpSchedule)	Upper Blue Nile Basin	
			Area (km ²)	% of Total Area
SHRB	Shrubland	AGRR	37,355.16	21.43
TEFF	Eragrostis Teff	TEFF/TEFF1	22,777.23	13.07
CRDY	Dryland cropland and pasture	AGRR	16,453.89	9.44
BWTF	Barley, Wheat and Teff	BARL/BARL1	15,841.12	9.09
GRSG	Grain Sorghum	CORN/CORN1	13,225.73	7.59
MIGS	Mixed Grassland/Shrubland	AGRR	12,212.19	7.01
FRSE	Forest-Evergreen	FRSE	8694.52	4.99
BARL	Spring Barley	BARL/BARL1	6057.46	3.48
BARR	Barren	SWRN	5895.60	3.38
CORN	Corn	CORN/CORN1	5288.42	3.03
FRST	Forest-Mixed	FRST	4812.12	2.76
COTF	Corn and Teff	CORN/CORN1	4540.01	2.60
PAST	Pasture	PAST	4040.28	2.32
WATR	Water	WATR	3364.04	1.93
BSVG	Barren or sparsely vegetated	SEWN	2896.77	1.66
BATF	Barley and Teff 50/50	TEFF/TEFF1	2559.19	1.47
FRSD	Forest-Deciduous	FRSD	2171.62	1.25
EUCA	Eucalyptus	FRST	1320.57	0.76
SGTF	Sorghum and Teff 50/50	TEFF/TEFF1	1141.82	0.66
RICE	Rice	RICE	799.52	0.46
SAVA	Savanna	AGRR	618.15	0.35
COFF	Coffee	AGRR	555.57	0.32
WETN	Wetlands-Non-Forested	WETN	490.08	0.28
TUHB	Herbaceous Tundra	AGRR	314.09	0.18
CPNM	Residential-Med/Low Density	AGRR	284.95	0.16
SUGC	Sugar cane	AGRR	152.56	0.09
URHD	Residential-High Density	AGRR	143.42	0.08
WEWO	Wooded Wetland	FRSE	112.86	0.06
TUMI	Mixed Tundra	FRSE	76.83	0.04
BANA	Bananas	AGRR	59.60	0.03
BACO	Bananas and Coffee	AGRR	31.69	0.02
TOTAL			174,287.05	100

Appendix C

DEM (30 × 30 m) of the upper Blue Nile basin.



Advanced Spaceborne Thermal Emission and Reflection Radiometer (ASTER) Global Digital Elevation Model Version 2 (GDEM V2) from the Ministry of Economy, Trade, and Industry (METI) of Japan and the United States National Aeronautics and Space Administration (NASA) of a 30 m resolution [51].

Appendix D

Land use, soil, and slope distribution for all seven sub-basins.

D1: Upper Abay sub-basin.

Upper Abay sub-basin				
MULTIPLE HRUs LandUse/Soil/Slope OPTION		THRESHOLDS : 0 / 0 / 0 [%]		
Number of HRUs: 13336				
Number of Subbasins: 64				
	Area [ha]	Area[acres]		
Watershed	4882982.9400	12066094.9939		
		Area [ha]	Area[acres]	%Wat.Area
LANDUSE:				
Spring Barley -->		BARL 443823.3155	1096709.6038	9.09
Barren -->		BARR 455264.4221	1124981.1502	9.32
Barley and Teff 50/50 -->		BATF 69114.6472	170785.7489	1.42
BAREN OR SPARSLY VEGETATED -->		BSVG 228180.4112	563845.2052	4.67
Barley, Wheat and Teff -->		BWTF 851361.4975	2103756.8284	17.44
Maiz and Teff -->		COTF 14220.6053	35139.8268	0.29
Forest-Mixed -->		FRST 107300.5381	265144.9948	2.20
Grain Sorghum -->		GRSG 465204.7885	1149544.2926	9.53
MIXED GRASSLAND/SHRUBLAND -->		MIGS 143223.2066	353911.7047	2.93
SHRUBLAND -->		SHRB 758135.2279	1873390.0549	15.53
Eragrostis Teff -->		TEFF 639047.5979	1579118.5668	13.09
Residential-Med/Low Density -->		URML 8314.2718	20544.9814	0.17
Dryland cropland and pasture -->		CRDY 501164.2888	1238402.0158	10.26
Pasture -->		PAST 89458.2545	221055.8198	1.83
Eucalyptus -->		EUCA 59747.1106	147638.0976	1.22
Residential-High Density -->		URHD 3950.1031	9760.9023	0.08
HERBACEOUS TUNDRA -->		TUHB 23530.4177	58144.8386	0.48
Water -->		WATR 720.3373	1779.9895	0.01
Mixed Tundra -->		TUMI 6185.3190	15284.2325	0.13
Wetlands-Non-Forested -->		WETN 3103.7811	7669.5983	0.06
Forest-Evergreen -->		FRSE 10731.2155	26517.3701	0.22
SAVANNA -->		SAVA 1184.7428	2927.5586	0.02
Rice -->		RICE 2.7917	6.8983	0.00
Forest-Deciduous -->		FRSD 14.0483	34.7141	0.00
SOILS:				
CMe	1114597.6330	2754226.4809	22.83	
LPe	45901.3976	113424.6486	0.94	
LPq	1958663.7230	4839955.9927	40.11	
NTu	80612.0372	199196.3744	1.65	
VRe	734881.7245	1815929.4852	15.05	
LVx	245101.0882	605657.0439	5.02	
LVh	111718.3787	276061.6997	2.29	
WR	46.2875	114.3786	0.00	
FLe	6770.3960	16729.9871	0.14	
LPk	225071.7672	556163.5905	4.61	
ARb	87661.3286	216615.5261	1.80	
CMv	271957.1786	672019.7861	5.57	
SLOPE:				
45-9999	1034342.5675	2555912.2015	21.18	
30-45	811091.3202	2004247.2068	16.61	
15-30	1415972.0211	3498937.6628	29.00	
0-15	1621577.0311	4006997.9228	33.21	

D2: Muger sub-basin.

Muger sub-basin			
MULTIPLE HRUs LandUse/Soil/Slope OPTION		THRESHOLDS : 0 / 0 / 0 [%]	
Number of HRUs: 8198			
Number of Subbasins: 41			
	Area [ha]	Area[acres]	
Watershed	726768.0000	1795880.0664	
LANDUSE:			
	Area [ha]	Area[acres]	%Wat.Area
Barren -->	BARR 14609.0228	36099.6259	2.01
BAREN OR SPARSLY VEGETATED -->	BSVG 753.7141	1862.4652	0.10
Barley, Wheat and Teff -->	BWTF 247502.8918	611592.0207	34.06
Forest-Evergreen -->	FRSE 671.0795	1658.2710	0.09
Forest-Mixed -->	FRST 11509.0988	28439.5586	1.58
Grain Sorghum -->	GRSG 1.8924	4.6762	0.00
MIXED GRASSLAND/SHRUBLAND -->	MIGS 19495.6386	48174.6977	2.68
SAVANNA -->	SAVA 154.9061	382.7807	0.02
SHRUBLAND -->	SHRB 68522.5594	169322.6703	9.43
Eragrostis Teff -->	TEFF 221740.7207	547932.4079	30.51
Dryland cropland and pasture -->	CRDY 21369.4706	52805.0302	2.94
Pasture -->	PAST 37540.6208	92764.7511	5.17
Eucalyptus -->	EUCA 2845.2617	7030.7839	0.39
Residential-High Density -->	URHD 712.9825	1761.8155	0.10
Residential-Med/Low Density -->	URML 1341.4381	3314.7605	0.18
Spring Barley -->	BARL 28464.3316	70336.7866	3.92
Barley and Teff 50/50 -->	BATF 49425.1349	122131.9795	6.80
Water -->	WATR 107.2357	264.9849	0.01
SOILS:			
FLe	8795.7641	21734.7729	1.21
LPk	243285.3730	601170.3210	33.47
LPq	65882.8479	162799.8112	9.07
LVx	67767.4935	167456.8649	9.32
NTh	23929.2509	59130.3754	3.29
NTu	123573.2453	305355.6678	17.00
ARb	85.3380	210.8745	0.01
VRe	111563.0222	275677.8059	15.35
CMv	66245.5570	163696.0836	9.12
CMe	2587.7157	6394.3748	0.36
LVh	13052.3924	32253.1142	1.80
SLOPE:			
45-9999	72057.5541	178057.8191	9.91
30-45	100979.3949	249525.1337	13.89
5-15	240470.1193	594213.6884	33.09
15-30	265027.8257	654897.0088	36.47
0-5	48233.1059	119186.4164	6.64

D3: Didesa sub-basin.

Didesa sub-basin				
MULTIPLE HRUs LandUse/Soil/Slope OPTION		THRESHOLDS : 0 / 0 / 0 [%]		
Number of HRUs: 8670				
Number of Subbasins: 54				
	Area [ha]	Area[acres]		
Watershed	2818926.9900	6965709.5386		
LANDUSE:				
	Area [ha]	Area[acres]	%Wat.Area	
Barren -->	BARR	6504.0456	16071.8219	0.23
Forest-Evergreen -->	FRSE	632589.2944	1563159.7759	22.44
Forest-Mixed -->	FRST	134376.9707	332052.2133	4.77
Grain Sorghum -->	GRSG	370568.1738	915692.4858	13.15
MIXED GRASSLAND/SHRUBLAND -->	MIGS	251562.2759	621622.9619	8.92
SAVANNA -->	SAVA	13743.7245	33961.4304	0.49
SHRUBLAND -->	SHRB	535935.5527	1324323.5475	19.01
Dryland cropland and pasture -->	CRDY	137329.8366	339348.8926	4.87
BAREN OR SPARSLY VEGETATED -->	BSVG	2801.4973	6922.6399	0.10
Barley, Wheat and Teff -->	BWTF	37016.8724	91470.5425	1.31
Corn -->	CORN	176873.9300	437064.3247	6.27
Eragrostis Teff -->	TEFF	57802.9527	142833.9863	2.05
Residential-Med/Low Density -->	URML	1999.1531	4940.0073	0.07
Forest-Deciduous -->	FRSD	11413.9171	28204.3598	0.40
Pasture -->	PAST	37668.3012	93080.2556	1.34
Eucalyptus -->	EUCA	23.7476	58.6816	0.00
Residential-High Density -->	URHD	1488.1255	3677.2325	0.05
Maiz and Teff -->	COTF	233859.4923	577878.4984	8.30
Sorghum and Teff 50/50 -->	SGTF	114975.3238	284109.7739	4.08
Wetlands-Non-Forested -->	WETN	5.9822	14.7824	0.00
Wooded Wetland -->	WEWO	763.0065	1885.4272	0.03
Water -->	WATR	227.9593	563.2988	0.01
Coffee -->	COFF	55933.3240	138214.0402	1.98
Banana and coffee -->	BACO	3187.6232	7876.7763	0.11
Bananas -->	BANA	275.9078	681.7819	0.01
SOILS:				
LPd	105949.0423	261805.3811	3.76	
NTu	2095065.1527	5177010.7456	74.32	
VRe	151023.2559	373186.0165	5.36	
WR	795.6368	1966.0584	0.03	
ALh	35817.7068	88507.3444	1.27	
CMv	23972.3439	59236.8604	0.85	
LPk	156368.9239	386395.4294	5.55	
LPq	21503.1324	53135.3153	0.76	
PHh	2185.8713	5401.3972	0.08	
CMe	8048.8210	19889.0392	0.29	
NTh	132928.9080	328473.9781	4.72	
ALu	84606.0706	209065.8308	3.00	
FLe	662.1243	1636.1422	0.02	
SLOPE:				
45-9999	161045.6696	397951.9019	5.71	
30-45	372039.2590	919327.6108	13.20	
5-15	1038263.1987	2565600.2773	36.83	
0-5	211029.8453	521465.2992	7.49	
15-30	1036549.0174	2561364.4494	36.77	

D4: Temcha sub-basin.

Temcha sub-basin			
MULTIPLE HRUs LandUse/Soil/Slope OPTION		THRESHOLDS : 0 / 0 / 0 [%]	
Number of HRUs: 4245			
Number of Subbasins: 23			
	Area [ha]	Area[acres]	
Watershed	552664.8000	1365662.3540	
	Area [ha]	Area[acres]	%Wat.Area
LANDUSE:			
Spring Barley -->	BARL 7238.5200	17886.7448	1.31
Barren -->	BARR 22242.0600	54961.2424	4.02
BAREN OR SPARSLY VEGETATED -->	BSVG 6753.0600	16687.1489	1.22
Barley, Wheat and Teff -->	BWTF 48592.9800	120075.6832	8.79
Maiz and Teff -->	COTF 5866.8300	14497.2303	1.06
Forest-Mixed -->	FRST 5067.6300	12522.3671	0.92
MIXED GRASSLAND/SHRUBLAND -->	MIGS 5788.3500	14303.3023	1.05
SHRUBLAND -->	SHRB 53432.1000	132033.3907	9.67
Eragrostis Teff -->	TEFF 195251.4900	482476.1944	35.33
Residential-Med/Low Density -->	URML 1587.5100	3922.8166	0.29
Dryland cropland and pasture -->	CRDY 85613.0400	211554.1025	15.49
Pasture -->	PAST 38467.2600	95054.5228	6.96
Sugarcane -->	SUGC 585.1800	1446.0090	0.11
Eucalyptus -->	EUCA 35250.4800	87105.6986	6.38
Residential-High Density -->	URHD 771.4800	1906.3657	0.14
Barley and Teff 50/50 -->	BATF 33858.4500	83665.9229	6.13
Forest-Evergreen -->	FRSE 1141.2000	2819.9623	0.21
Water -->	WATR 181.3500	448.1249	0.03
HERBACEOUS TUNDRA -->	TUHB 2846.8800	7034.7828	0.52
Mixed Tundra -->	TUMI 747.0000	1845.8744	0.14
SAVANNA -->	SAVA 1381.9500	3414.8675	0.25
SOILS:			
LPq	70773.4800	174884.8078	12.81
LVx	155910.0600	385261.5538	28.21
NTu	160212.1500	395892.2333	28.99
VRe	156875.8500	387648.0691	28.39
CMe	891.5400	2203.0399	0.16
LPk	8001.7200	19772.6502	1.45
SLOPE:			
30-45	58719.3300	145098.4004	10.62
15-30	168574.0500	416554.9063	30.50
0-5	57253.5000	141476.2612	10.36
45-9999	41599.0800	102793.4066	7.53
5-15	226518.8400	559739.3796	40.99

D5: Dabus sub-basin.

Dabus sub-basin				
MULTIPLE HRUs LandUse/Soil/Slope OPTION		THRESHOLDS : 0 / 0 / 0 [%]		
Number of HRUs: 2521				
Number of Subbasins: 15				
	Area [ha]	Area[acres]		
Watershed	1474193.1600	3642805.0080		
LANDUSE:				
		Area [ha]	Area[acres]	%Wat.Area
BAREN OR SPARSLY VEGETATED -->	BSVG	1709.3382	4223.8602	0.12
Forest-Mixed -->	FRST	37901.9669	93657.6553	2.57
MIXED GRASSLAND/SHRUBLAND -->	MIGS	83794.5141	207060.4341	5.68
SHRUBLAND -->	SHRB	302129.3456	746576.7195	20.49
Forest-Deciduous -->	FRSD	32028.3466	79143.6458	2.17
Dryland cropland and pasture -->	CRDY	185965.6108	459530.3226	12.61
Barren -->	BARR	1271.7296	3142.5073	0.09
Barley, Wheat and Teff -->	BWTF	31112.9361	76881.6208	2.11
Grain Sorghum -->	GRSG	136751.4830	337919.7520	9.28
Corn -->	CORN	304439.0522	752284.1199	20.65
Forest-Evergreen -->	FRSE	127174.8535	314255.4218	8.63
Residential-Med/Low Density -->	URML	2424.0538	5989.9583	0.16
Pasture -->	PAST	55508.1053	137163.3037	3.77
Residential-High Density -->	URHD	2868.7076	7088.7199	0.19
Wooded Wetland -->	WEWO	10296.6741	25443.5964	0.70
Maiz and Teff -->	COTF	155967.2445	385402.8595	10.58
Wetlands-Non-Forested -->	WETN	2828.6047	6989.6238	0.19
Water -->	WATR	20.5933	50.8872	0.00
SOILS:				
NTu	934227.3532	2308522.5011	63.37	
VRe	202556.2624	500526.6521	13.74	
ALh	74731.9958	184666.4982	5.07	
LPd	59032.8194	145873.0485	4.00	
WR	160.0501	395.4917	0.01	
HSf	1037.1641	2562.8844	0.07	
CMe	3813.0210	9422.1655	0.26	
NTh	173452.9841	428610.9964	11.77	
ALu	25181.5099	62224.7701	1.71	
SLOPE:				
30-45	113439.6323	280315.0033	7.70	
15-30	496825.9038	1227681.6495	33.70	
5-15	671930.3299	1660373.4417	45.58	
0-5	154192.3327	381016.9637	10.46	
45-9999	37804.9614	93417.9498	2.56	

D6: Beles sub-basin.

Area [ha]		Area[acres]		
Watershed	352663.7400	871449.7347		
LANDUSE:				
	Area [ha]	Area[acres]	%Wat.Area	
Barren -->	BARR	1031.8573	2549.7709	0.29
BAREN OR SPARSLY VEGETATED -->	BSVG	3007.6182	7431.9750	0.85
Forest-Mixed -->	FRST	4035.6945	9972.4029	1.14
Grain Sorghum -->	GRSG	54718.0542	135211.0478	15.52
MIXED GRASSLAND/SHRUBLAND -->	MIGS	35482.5851	87679.2419	10.06
SHRUBLAND -->	SHRB	149472.8373	369354.8545	42.38
Water -->	WATR	236.0434	583.2751	0.07
Dryland cropland and pasture -->	CRDY	61285.4990	151439.5324	17.38
Pasture -->	PAST	3567.8388	8816.3080	1.01
Barley, Wheat and Teff -->	BWTF	3590.6149	8872.5889	1.02
Eragrostis Teff -->	TEFF	35571.7991	87899.6941	10.09
Residential-Med/Low Density -->	URML	264.4011	653.3482	0.07
Wetlands-Non-Forested -->	WETN	2.7907	6.8961	0.00
Residential-High Density -->	URHD	144.9389	358.1514	0.04
Maiz and Teff -->	COTF	1.3504	3.3368	0.00
Eucalyptus -->	EUCA	29.6180	73.1875	0.01
Wooded Wetland -->	WEWO	0.6302	1.5572	0.00
SAVANNA -->	SAVA	219.5690	542.5660	0.06
SOILS:				
LPe	49072.4571	121260.4950	13.91	
LVh	55922.3978	138187.0411	15.86	
NTu	40773.7570	100753.9922	11.56	
VRe	163973.4840	405186.6776	46.50	
CMe	29224.2833	72214.6653	8.29	
LPq	13623.7211	33664.8959	3.86	
LPk	73.6398	181.9676	0.02	
SLOPE:				
0-5	39999.6390	98841.1078	11.34	
5-15	150128.3034	370974.5442	42.57	
45-9999	29225.4536	72217.5572	8.29	
30-45	36960.6923	91331.7187	10.48	
15-30	96349.6517	238084.8068	27.32	

D7: Lower Abay sub-basin.

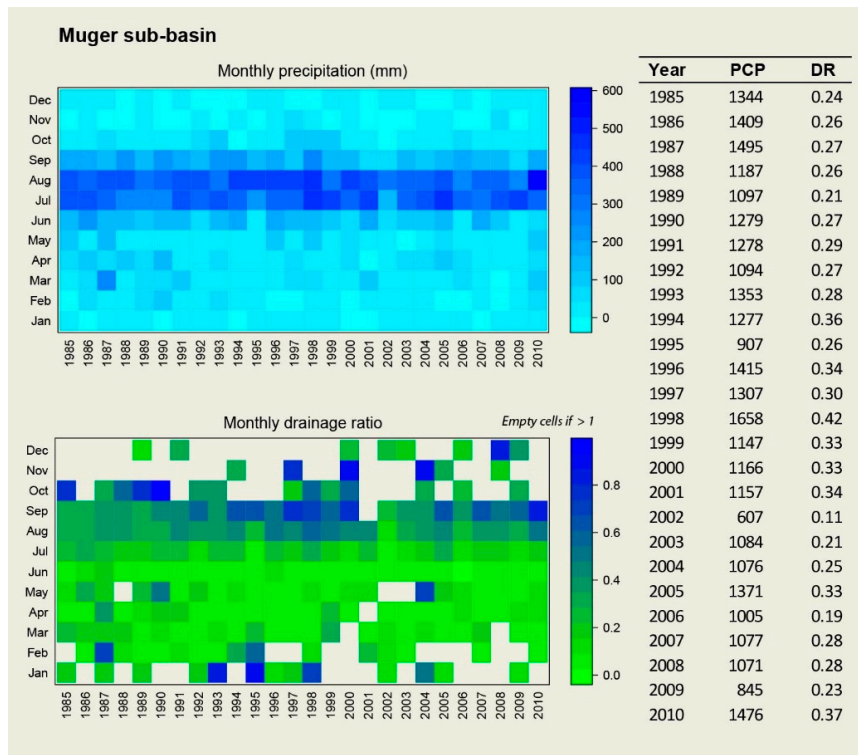
Lower Abay sub-basin			
MULTIPLE HRUs LandUse/Soil/Slope OPTION		THRESHOLDS : 0 / 0 / 0 [%]	
Number of HRUs: 22026			
Number of Subbasins: 116			
	Area [ha]	Area[acres]	
Watershed	5101083.3600	12605032.0367	
	Area [ha]	Area[acres]	%Wat.Area
LANDUSE:			
Barren -->	BARR 51732.8731	127834.5161	1.01
BAREN OR SPARSLY VEGETATED -->	BSVG 29730.7883	73466.2643	0.58
Barley, Wheat and Teff -->	BWTF 219712.7306	542921.1430	4.31
Forest-Mixed -->	FRST 150362.9148	371554.2806	2.95
Grain Sorghum -->	GRSG 299921.3250	741120.5902	5.88
MIXED GRASSLAND/SHRUBLAND -->	MIGS 684193.6161	1690676.6352	13.41
SHRUBLAND -->	SHRB 1793550.6100	4431953.2349	35.16
Residential-Med/Low Density -->	URML 5203.0235	12856.9313	0.10
Forest-Deciduous -->	FRSD 174477.8072	431143.3854	3.42
Dryland cropland and pasture -->	CRDY 491946.2987	1215623.9014	9.64
Residential-High Density -->	URHD 2169.1165	5359.9954	0.04
Forest-Evergreen -->	FRSE 101994.1201	252032.5704	2.00
SAVANNA -->	SAVA 46062.5663	113822.9043	0.90
Pasture -->	PAST 71136.3385	175781.4491	1.39
Maiz and Teff -->	COTF 12010.7178	29679.0843	0.24
Eragrostis Teff -->	TEFF 643996.3142	1591347.0922	12.62
Water -->	WATR 26103.0609	64501.9686	0.51
Eucalyptus -->	EUCA 16578.6157	40966.5882	0.33
Corn -->	CORN 50018.8381	123599.0499	0.98
Barley and Teff 50/50 -->	BATF 89809.6849	221924.2219	1.76
Wetlands-Non-Forested -->	WETN 16733.4428	41349.1738	0.33
Wooded Wetland -->	WEWO 269.1624	665.1138	0.01
Spring Barley -->	BARL 102202.9966	252548.7148	2.00
HERBACEOUS TUNDRA -->	TUHB 2636.4902	6514.8992	0.05
Mixed Tundra -->	TUMI 69.2339	171.0803	0.00
Sugarcane -->	SUGC 12764.2461	31541.0903	0.25
Bananas -->	BANA 5696.4277	14076.1577	0.11
SOILS:			
WR	38097.0577	94139.7345	0.75
LPd	291153.4811	719454.8095	5.71
NTu	2610838.3560	6451512.1196	51.18
ALh	270113.4395	667463.8147	5.30
LPe	9909.2083	24486.1491	0.19
LVx	149521.5337	369475.1858	2.93
VRe	481134.8811	1188908.3480	9.43
CMe	67431.3331	166626.1956	1.32
LPq	217910.3908	538467.4712	4.27
LVh	20874.0972	51580.9380	0.41
FLe	95357.6123	235633.4280	1.87
LPk	705691.7219	1743799.5294	13.83
PHh	130787.5398	323182.5502	2.56
ARb	2341.7492	5786.5794	0.05
CMv	3.1634	7.8170	0.00
NTh	7550.0150	18656.4646	0.15
HSf	1437.2803	3551.5916	0.03
VRd	930.4994	2299.3105	0.02
SLOPE:			
5-15	1951650.5436	4822626.0757	38.26
0-5	483212.8006	1194042.9909	9.47
45-9999	468215.8079	1156984.6721	9.18
30-45	623469.1093	1540623.3425	12.22
15-30	1574535.0987	3890754.9556	30.87

Appendix E

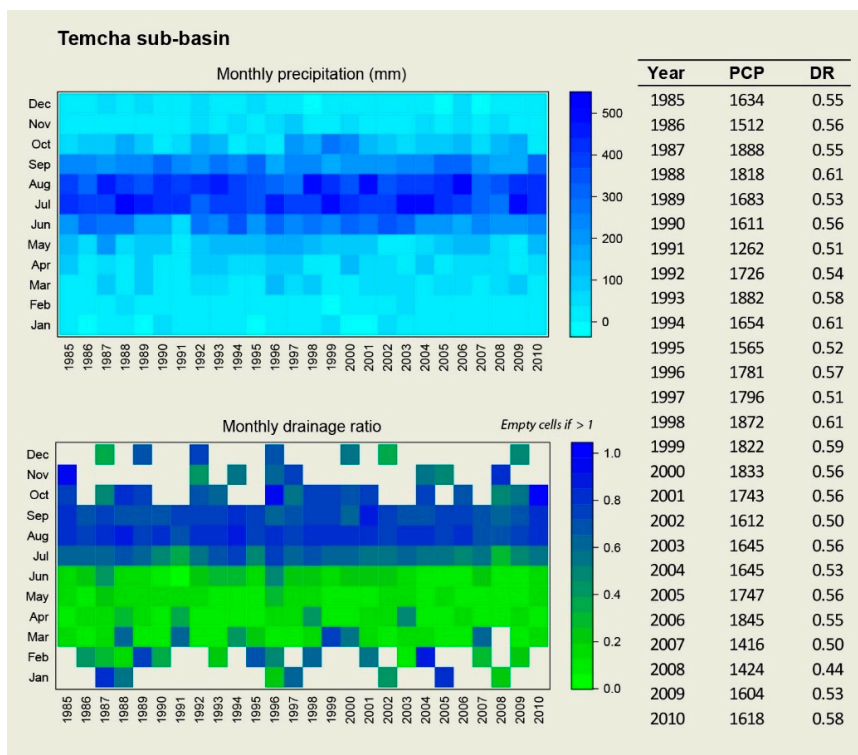
Monthly and annual distribution of precipitation and rainfall for all seven sub-basins *.

* Upper Abay sub-basin see Figure 7.

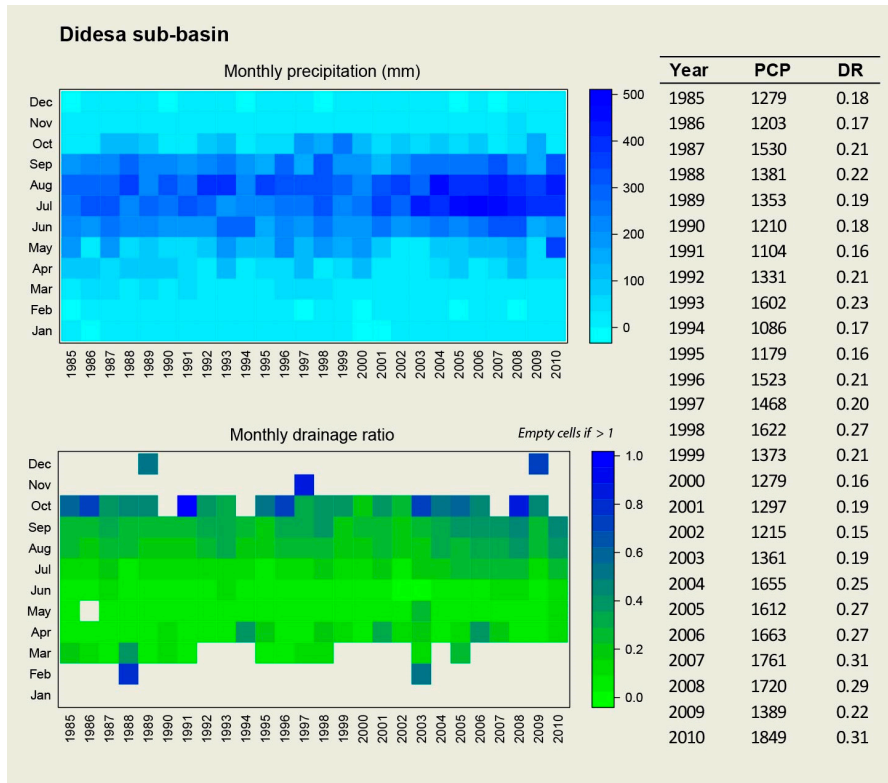
E1: Muger sub-basin.



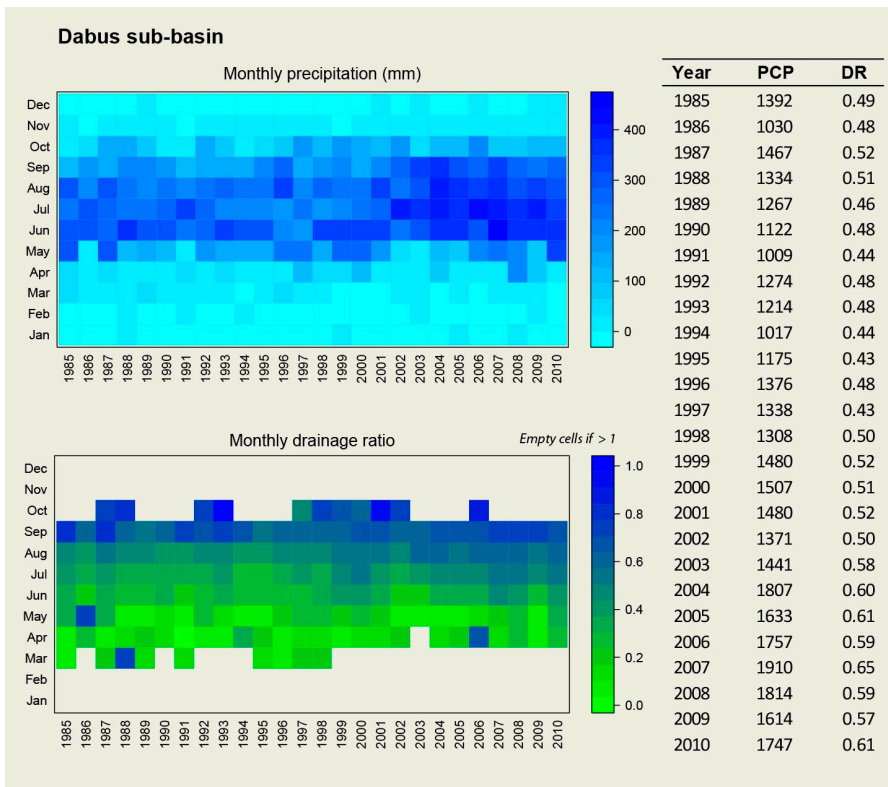
E2: Temcha sub-basin.



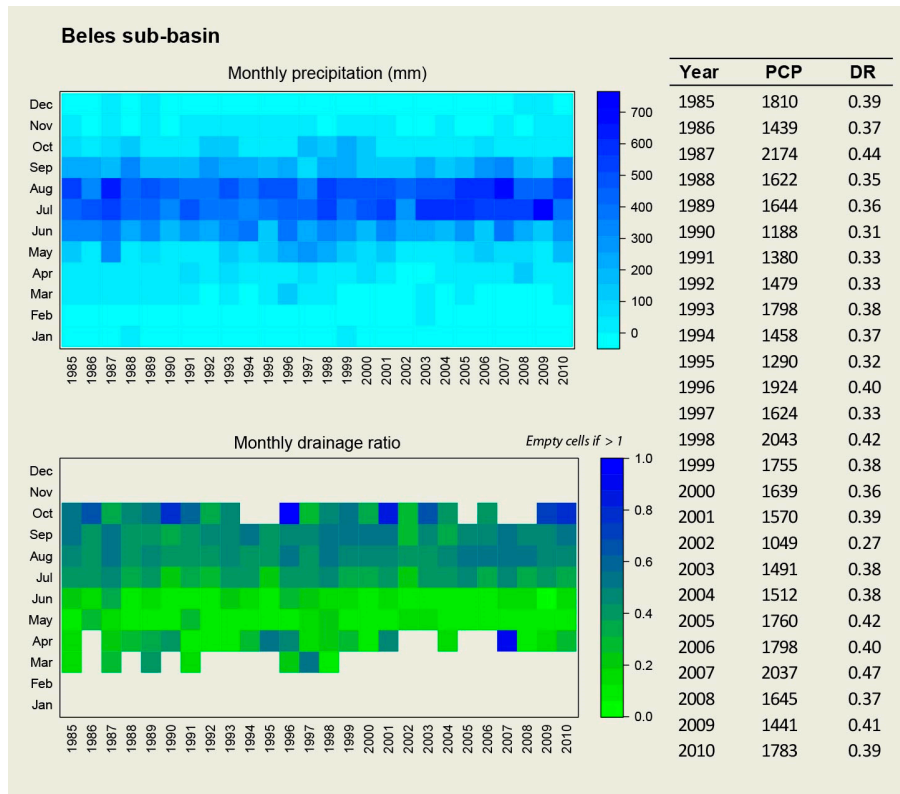
E3: Didesa sub-basin.



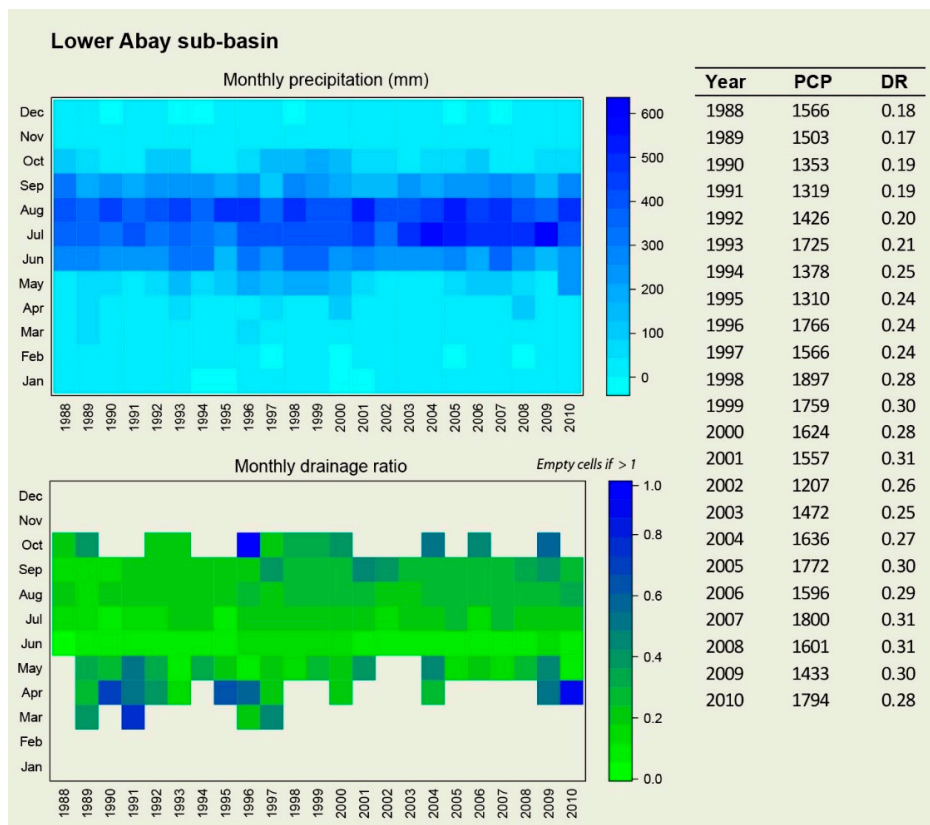
E4. Dabus sub-basin.



E5: Beles sub-basin.



E6: Lower Abay sub-basin.



Appendix F

Description of input parameters selected for discharge calibration, final parameter ranges after calibration (Min, Max), and parameters giving the best objective function in the calibration process (Best Sim).

SWAT Parameter	Description	Upper Abay			Muger			Temcha			Didesa			Beles			Dabus			Lower Abay		
		Best Sim	Min	Max	Best Sim	Min	Max	Best Sim	Min	Max	Best Sim	Min	Max	Best Sim	Min	Max	Best Sim	Min	Max	Best Sim	Min	Max
A__CN2.mgt	SCS runoff curve number for moisture condition II	4.4	-8	8	-2.1	-9	9	2.2	-7	10	-3.8	-6	5	1.8	-12	4	-5.1	-6	6	-9.6	-10	10
V__GW_DELAY.gw	Groundwater delay (days)	9	1	60	15	10	400	6	1	100	42	40	250	46	0	80	67	60	100	345	70	500
V__GWQMN.gw	Threshold depth of water in the shallow aquifer required for return flow to occur (mm)	2865	100	4000	4298	3000	5000	936	500	4500	2073	1000	3500	3150	3000	5000	2438	2000	2500	4644	4000	5000
V__GW_REVAP.gw	Groundwater "revap" coefficient	0.17	0.03	0.19	0.19	0.19	0.2	0.03	0.02	0.2	0.18	0.175	0.19	0.16	0.15	0.2	0.06	0.05	0.08	0.195	0.17	0.2
V__CH_K2.rte	Effective hydraulic conductivity in main channel alluvium (mm/hr)	134	0	200	428	200	500	158	0	300	33	10	190	205	0	300	228	100	300	363	150	500
V__RCHRG_DP.gw	Deep aquifer percolation fraction	0.104	0	0.3	0.020	0.01	0.1	0.110	0.01	0.2	0.124	0.1	0.6	0.113	0	0.3	0.028	0	0.1	0.112	0	0.2
R__SOL_AWC().sol	Available water capacity of the soil layer	0.26	-0.5	0.7	0.92	0.5	2	0.56	-1	1.5	0.25	0.2	0.9	0.37	0	1	0.03	0.02	0.1	1.79	0.5	2.5
V__CH_N2.rte	Manning's "n" value for the main channel	0.04	0.03	0.15	0.14	0.05	0.15	0.15	0.05	0.2	0.13	0.075	0.15	0.24	0.01	0.25	0.10	0.05	0.15	0.06	0.05	1.5
V__ALPHA_BF.gw	Baseflow alpha factor	0.30	0.1	0.8	0.49	0.1	0.5	0.88	0.7	0.95	0.40	0.1	0.6	0.24	0.2	0.7	0.08	0.07	0.1	0.75	0.6	1
R__SOL_K().sol	Saturated hydraulic conductivity (mm/hr)	0.95	0	2	1.21	0	2	0.02	-1	2	1.40	0.75	1.8	0.95	-0.5	2	0.62	0.4	0.8	0.65	0	2
V__REVAPMN.gw	Threshold depth of water in the shallow aquifer required for "revap" to occur (mm)	244	1	350	234	50	300	*	*	*	22	10	85	24	1	210	50	50	100	332	50	500
V__ESCO.bsn	Soil evaporation compensation factor	*	*	*	*	*	*	*	*	*	*	*	*	0.77	0.6	0.95	0.87	0.8	0.95	*	*	*
V__SURLAG.bsn	Surface runoff lag coefficient	*	*	*	*	*	*	*	*	*	*	*	*	5.52	1	12	2.34	1	5	*	*	*

Note: In the parameter names, A__ means the given value is added to the existing parameter value; r__ means the existing parameter value is multiplied by (1 + a given value); v__ means the existing parameter value is to be replaced by the given value [67]. *After sensitivity analysis, these insensitive parameters were excluded for the final calibration.

References

1. Conway, D. From headwater tributaries to international river: Observing and adapting to climate variability and change in the Nile basin. *Glob. Environ. Chang.* **2005**, *15*, 99–114. [[CrossRef](#)]
2. Khadr, M. Forecasting of meteorological drought using Hidden Markov Model (case study: The upper Blue Nile river basin, Ethiopia). *Ain Shams Eng. J.* **2016**, *7*, 47–56. [[CrossRef](#)]
3. Mohamed, A.A.A.; Mohamed, A.A.A.; Ahmed, M.S.M.; Abdrabbo, M.A.A. Trend of Change in Cultivated Area and Water Budget for Major Crops in Egypt using GIS and Field Survey Technique. *J. Agric. Inform.* **2015**, *6*, 42–56. [[CrossRef](#)]
4. Hagos, F.; Makombe, G.; Namara, R.E.; Awulachew, S.B. *Importance of Irrigated Agriculture to the Ethiopian Economy: Capturing the Direct Net Benefits of Irrigation*; International Water Management Institute (IMWI): Colombo, Sri Lanka, 2009.
5. Rockström, J.; Lannerstad, M.; Falkenmark, M. Assessing the water challenge of a new green revolution in developing countries. *Proc. Natl. Acad. Sci. USA* **2007**, *104*, 6253–6260. [[CrossRef](#)] [[PubMed](#)]
6. Gebremicael, T.G.; Mohamed, Y.A.; Betrie, G.D.; van der Zaag, P.; Teferi, E. Trend analysis of runoff and sediment fluxes in the Upper Blue Nile basin: A combined analysis of statistical tests, physically-based models and landuse maps. *J. Hydrol.* **2013**, *482*, 57–68. [[CrossRef](#)]
7. Tesemma, Z.K.; Mohamed, Y.A.; Steenhuis, T.S. Trends in rainfall and runoff in the Blue Nile Basin: 1964–2003. *Hydrol. Process.* **2010**, *24*, 3747–3758. [[CrossRef](#)]
8. Mengistu, D.T.; Sorteberg, A. Sensitivity of SWAT simulated streamflow to climatic changes within the Eastern Nile River basin. *Hydrol. Earth Syst. Sci.* **2012**, *16*, 391–407. [[CrossRef](#)]
9. Koch, M.; Cherie, N. SWAT-Modeling of the Impact of future Climate Change on the Hydrology and the Water Resources in the Upper Blue Nile River Basin, Ethiopia. In Proceedings of the ICWRER 2013—6th International Conference on Water Resources and Environment Research, Koblenz, Germany, 3–7 June 2013; Volume 6, pp. 488–523.
10. Easton, Z.M.; Fuka, D.R.; White, E.D.; Collick, A.S.; Biruk Ashagre, B.; McCartney, M.; Awulachew, S.B.; Ahmed, A.A.; Steenhuis, T.S. A multi basin SWAT model analysis of runoff and sedimentation in the Blue Nile, Ethiopia. *Hydrol. Earth Syst. Sci.* **2010**, *14*, 1827–1841. [[CrossRef](#)]
11. Kim, U.; Kaluarachchi, J.J. Application of parameter estimation and regionalization methodologies to ungauged basins of the Upper Blue Nile River Basin, Ethiopia. *J. Hydrol.* **2008**, *362*, 39–56. [[CrossRef](#)]
12. Tekleab, S.; Uhlenbrook, S.; Mohamed, Y.; Savenije, H.H.G.; Temesgen, M.; Wenninger, J. Water balance modeling of Upper Blue Nile catchments using a top-down approach. *Hydrol. Earth Syst. Sci.* **2011**, *15*, 2179–2193. [[CrossRef](#)]
13. Haregeweyn, N.; Tsunekawa, A.; Poesen, J.; Tsubo, M.; Meshesha, D.T.; Fenta, A.A.; Nyssen, J.; Adgo, E. Comprehensive assessment of soil erosion risk for better land use planning in river basins: Case study of the Upper Blue Nile River. *Sci. Total Environ.* **2017**, *574*, 95–108. [[CrossRef](#)] [[PubMed](#)]
14. Betrie, G.D.; Mohamed, Y.A.; van Griensven, A.; Srinivasan, R. Sediment management modelling in the Blue Nile Basin using SWAT model. *Hydrol. Earth Syst. Sci.* **2011**, *15*, 807–818. [[CrossRef](#)]
15. Steenhuis, T.S.; Collick, A.S.; Easton, Z.M.; Leggesse, E.S.; Bayabil, H.K.; White, E.D.; Awulachew, S.B.; Adgo, E.; Ahmed, A.A. Predicting discharge and sediment for the Abay (Blue Nile) with a simple model. *Hydrol. Process.* **2009**, *23*, 3728–3737. [[CrossRef](#)]
16. Conway, D. A water balance model of the Upper Blue Nile in Ethiopia. *Hydrol. Sci. J.* **1997**, *42*, 265–286. [[CrossRef](#)]
17. Ali, Y.S.A.; Crosato, A.; Mohamed, Y.A.; Abdalla, S.H.; Wright, N.G. Sediment balances in the Blue Nile River Basin. *Int. J. Sediment Res.* **2014**, *29*, 316–328. [[CrossRef](#)]
18. Allam, M.M.; Jain Figueroa, A.; McLaughlin, D.B.; Eltahir, E.A.B. Estimation of evaporation over the upper Blue Nile basin by combining observations from satellites and river flow gauges. *Water Resour. Res.* **2016**, *52*, 644–659. [[CrossRef](#)]
19. Abera, W.; Brocca, L.; Rigon, R. Comparative evaluation of different satellite rainfall estimation products and bias correction in the Upper Blue Nile (UBN) basin. *Atmos. Res.* **2016**, *178*, 471–483. [[CrossRef](#)]
20. Geza, M.; McCray, J.E. Effects of soil data resolution on SWAT model stream flow and water quality predictions. *J. Environ. Manag.* **2008**, *88*, 393–406. [[CrossRef](#)]

21. Tsidu, G.M. High-resolution monthly rainfall database for Ethiopia: Homogenization, reconstruction, and gridding. *J. Clim.* **2012**, *25*, 8422–8443. [[CrossRef](#)]
22. Berhane, S.; Zemadim, B.; Melesse, A.M. *Rainfall–Runoff Processes and Modeling: The Case of Meja Watershed in the Upper Blue Nile Basin of Ethiopia*; Springer International Publishing: Cham, Switzerland, 2016; pp. 183–206.
23. Dessie, M.; Verhoest, N.E.C.; Pauwels, V.R.N.; Admasu, T.; Poesen, J.; Adgo, E.; Deckers, J.; Nyssen, J. Analyzing runoff processes through conceptual hydrological modelling in the Upper Blue Nile basin, Ethiopia. *Hydrol. Earth Syst. Sci.* **2014**, *11*, 5149–5167. [[CrossRef](#)]
24. Enku, T.; Melesse, A.M.; Ayana, E.K.; Tilahun, S.A.; Zeleke, G.; Steenhuis, T.S. Watershed Storage Dynamics in the Upper Blue Nile Basin: The Anjeni Experimental Watershed, Ethiopia. In *Landscape Dynamics, Soils and Hydrological Processes in Varied Climates*; Melesse, A.M., Abtew, W., Eds.; Springer International Publishing: Cham, Switzerland, 2016; pp. 261–277.
25. Lemann, T.; Zeleke, G.; Amsler, C.; Giovanoli, L.; Suter, H.; Roth, V. Modelling the effect of soil and water conservation on discharge and sediment yield in the upper Blue Nile basin, Ethiopia. *Appl. Geogr.* **2016**, *73*, 89–101. [[CrossRef](#)]
26. Roth, V.; Nigusie, T.K.T.K.; Lemann, T. Model parameter transfer for streamflow and sediment loss prediction with SWAT in a tropical watershed. *Environ. Earth Sci.* **2016**, *75*, 1321. [[CrossRef](#)]
27. Tekleab, S.; Uhlenbrook, S.; Savenije, H.H.G.; Mohamed, Y.; Wenninger, J. Modelling rainfall–runoff processes of the Chemoga and Jedeb meso-scale catchments in the Abay/Upper Blue Nile basin, Ethiopia. *Hydrol. Sci. J.* **2015**, *60*, 2029–2046. [[CrossRef](#)]
28. Tilahun, S.A.; Guzman, C.D.; Zegeye, A.D.; Engda, T.A.; Collick, A.S.; Rimmer, A.; Steenhuis, T.S. An efficient semi-distributed hillslope erosion model for the subhumid Ethiopian Highlands. *Hydrol. Earth Syst. Sci.* **2013**, *17*, 1051–1063. [[CrossRef](#)]
29. Woldeesenbet, T.A.; Elagib, N.A.; Ribbe, L.; Heinrich, J. Hydrological responses to land use/cover changes in the source region of the Upper Blue Nile Basin, Ethiopia. *Sci. Total Environ.* **2017**, *575*, 724–741. [[CrossRef](#)] [[PubMed](#)]
30. Lemann, T.; Roth, V.; Zeleke, G. Impact of precipitation and temperature changes on hydrological responses of small-scale catchments in the Ethiopian Highlands. *Hydrol. Sci. J.* **2016**, *62*, 270–282. [[CrossRef](#)]
31. Gassman, P.W.; Reyes, M.R.; Green, C.H. *Arnold The Soil and Water Assessment Tool: Historical Development, Applications, and Future Research Directions*; Center for Agricultural and Rural Development, Iowa State University: Ames, IA, USA, 2007.
32. Abbaspour, K.C.; Johnson, C.A.; van Genuchten, M.T. Estimating uncertain flow and transport parameters using a sequential uncertainty fitting procedure. *Vadose Zone J.* **2004**, *3*, 1340–1352. [[CrossRef](#)]
33. Abbaspour, K.C.; Yang, J.; Maximov, I.; Siber, R.; Bogner, K.; Mieleitner, J.; Zobrist, J.; Srinivasan, R. Modelling hydrology and water quality in the pre-alpine/alpine Thur watershed using SWAT. *J. Hydrol.* **2007**, *333*, 413–430. [[CrossRef](#)]
34. Awulachew, S.B.; McCartney, M.; Steenhuis, T.S.; Ahmed, A.A. *A Review of Hydrology, Sediment and Water Resource Use in the Blue Nile Basin*; Working Paper 131; International Water Management Institute (IWMI): Colombo, Sri Lanka, 2009.
35. Haile, A.T.; Rientjes, T.; Gieske, A.; Gebremichael, M. Rainfall Variability over Mountainous and Adjacent Lake Areas: The Case of Lake Tana Basin at the Source of the Blue Nile River. *J. Appl. Meteorol. Climatol.* **2009**, *48*, 1696–1717. [[CrossRef](#)]
36. Dessie, M.; Verhoest, N.E.C.; Pauwels, V.R.N.; Adgo, E.; Deckers, J.; Poesen, J.; Nyssen, J. Water balance of a lake with floodplain buffering: Lake Tana, Blue Nile Basin, Ethiopia. *J. Hydrol.* **2015**, *522*, 174–186. [[CrossRef](#)]
37. Berehanu, B.; Azagegn, T.; Ayenew, T.; Masetti, M. Inter-Basin Groundwater Transfer and Multiple Approach Recharge Estimation of the Upper Awash Aquifer System. *J. Geosci. Environ. Prot.* **2017**, *5*, 76–98. [[CrossRef](#)]
38. Azagegn, T.; Asrat, A.; Ayenew, T.; Kebede, S. Litho-structural control on interbasin groundwater transfer in central Ethiopia. *J. Afr. Earth Sci.* **2015**, *101*, 383–395. [[CrossRef](#)]
39. WLRC Water and Land Resources Information System (WALRIS). Available online: <http://walris.wlrc-eth.org/> (accessed on 22 May 2017).
40. Neitsch, S.L.; Arnold, J.G.; Kiniry, J.R.; Williams, J.R. *Soil & Water Assessment Tool Theoretical Documentation, Version 2009*; Texas Water Resources Institute: College Station, TX, USA, 2011.
41. Hargreaves, G.L.; Hargreaves, G.H.; Riley, J.P. Agricultural Benefits for Senegal River Basin. *J. Irrig. Drain. Eng.* **1985**, *111*, 113–124. [[CrossRef](#)]

42. Arnold, J.G.; Allen, P.M.; Muttiah, R.; Bernhardt, G. Automated Base Flow Separation and Recession Analysis Techniques. *Ground Water* **1995**, *33*, 1010–1018. [[CrossRef](#)]
43. Arnold, J.G.; Moriasi, D.N.; Gassman, P.W.; Abbaspour, K.C.; White, M.J.; Srinivasan, R.; Santhi, C.; Harmel, R.D.; van Griensven, A.; Van Liew, M.W.; et al. SWAT: Model Use, Calibration, and Validation. *Trans. ASABE* **2012**, *55*, 1491–1508. [[CrossRef](#)]
44. Stehr, A.; Debels, P.; Arumi, J.L.; Romero, F.; Alcayaga, H. Combining the Soil and Water Assessment Tool (SWAT) and MODIS imagery to estimate monthly flows in a data-scarce Chilean Andean basin. *Hydrol. Sci. J.* **2009**, *54*, 1053–1067. [[CrossRef](#)]
45. Gessesse, B.; Bewket, W.; Bräuning, A. Model-based characterization and monitoring of runoff and soil erosion in response to land use/land cover changes in the Modjo watershed, Ethiopia. *Land. Degrad. Dev.* **2014**, *26*, 711–724. [[CrossRef](#)]
46. Tibebe, D.; Bewket, W. Surface runoff and soil erosion estimation using the SWAT model in the Keleta Watershed, Ethiopia. *Land. Degrad. Dev.* **2011**, *22*, 551–564. [[CrossRef](#)]
47. Lin, S.; Jing, C.; Chaplot, V.; Yu, X.; Zhang, Z.; Moore, N.; Wu, J. Effect of DEM resolution on SWAT outputs of runoff, sediment and nutrients. *Hydrol. Earth Syst. Sci. Discuss.* **2010**, *7*, 4411–4435. [[CrossRef](#)]
48. Setegn, S.G.; Dargahi, B.; Srinivasan, R.; Melesse, A.M. Modeling of Sediment Yield From Anjeni-Gauged Watershed, Ethiopia Using SWAT Model. *J. Am. Water Resour. Assoc.* **2010**, *46*, 514–526. [[CrossRef](#)]
49. Stehr, A.; Debels, P.; Romero, F.; Alcayaga, H. Hydrological modelling with SWAT under conditions of limited data availability: Evaluation of results from a Chilean case study. *Hydrol. Sci. J.* **2008**, *53*, 588–601. [[CrossRef](#)]
50. Schuol, J.; Abbaspour, K.C. Using monthly weather statistics to generate daily data in a SWAT model application to West Africa. *Ecol. Modell.* **2007**, *201*, 301–311. [[CrossRef](#)]
51. Tachikawa, T.; Kaku, M.; Iwasaki, A.; Gesch, D. *ASTER Global Digital Elevation Model Version 2-Summary of Validation Results*; NASA: Washington, DC, USA, 2011.
52. Abbay River Basin Integrated Development Master Plan Project, Executive Summary. In *Abbay Master Plan Project*; Ministry of Water Resource (MoWR), The Federal Democratic Republic of Ethiopia, BCEOM French Engineering Consultants in Association with ISL and BRGM: Addis Ababa, Ethiopia, 1999.
53. Tegegne, G.; Hailu, D.I.D.; Aranganathan, P.D.S.M. Evaluation of Operation of Lake Tana Reservoir Future Water Use under Emerging Scenario with and without climate Change Impacts, Upper Blue Nile. *Int. J. Comput. Technol.* **2013**, *4*, 654–663. [[CrossRef](#)]
54. Setegn, S.G.; Srinivasan, R.; Melesse, A.M.; Dargahi, B. SWAT model application and prediction uncertainty analysis in the Lake Tana Basin, Ethiopia. *Hydrol. Process.* **2009**, *24*, 357–367. [[CrossRef](#)]
55. Setegn, S.G.; Srinivasan, R.; Dargahi, B.; Melesse, A.M. Spatial delineation of soil erosion vulnerability in the Lake Tana Basin, Ethiopia—10.1002_hyp.pdf. *Hydrol. Process.* **2009**, *24*, 357–367.
56. Kassawmar, T.; Eckert, S.; Zeleke, G.; Hurni, H. Reducing Landscape Heterogeneity for Improved Land Use and Land Cover (LULC) Classification over Large and Complex Ethiopian Highlands. *Geocarto Int.* **2018**, *33*, 53–69. [[CrossRef](#)]
57. Hurni, K.; Zeleke, G.; Kassie, M.; Tegegne, B.; Kassawmar, T.; Teferi, E.; Moges, A.; Tadesse, D.; Ahmed, M.; Degu, Y.; et al. *Economics of Land Degradation (ELD) Ethiopia Case Study: Soil Degradation and Sustainable Land Management in the Rainfed Agricultural Areas of Ethiopia: An Assessment of the Economic Implications 2015*; Water and Land Resource Centre (WLRC): Addis Abeba, Ethiopia; Centre for Development and Environment (CDE): Bern, Switzerland; Deutsche Gesellschaft für Internationale Zusammenarbeit (GIZ): Bonn, German, 2015. [[CrossRef](#)]
58. Medhin, G. *Livelihood Zones Analysis—A Tool for Planning Agricultural Water Management Investments*; FAOWATER: Addis Abeba, Ethiopia, 2011.
59. Hurni, H. *Agroecological Belts of Ethiopia Explanatory Notes on Three Maps at a Scale of 1:1,000,00*. *Soil Conservation Research Programme, Research Report 43*; Centre for Development and Environment, University of Bern, Switzerland: Addis Abeba, Ethiopia; Bern, Switzerland, 1998.
60. Loetscher, M. Status und Dynamik der Landwirtschaftlichen Produktion und Produktivität in einem Kleinzugsgebiet in Maybar, Wello, Äthiopien. Master's Thesis, University of Bern, Bern, Switzerland, 2003.
61. Ludi, E. Household and communal strategies dealing with degradation of and conflicts over natural resources: Case studies from the Ethiopian highlands. *Transform. Resour. Confl. Approach Instrum.* **2002**, 19–92.

62. Dile, Y.T.; Srinivasan, R. Evaluation of CFSR climate data for hydrologic prediction in data-scarce watersheds: An application in the Blue Nile River Basin. *J. Am. Water Resour. Assoc.* **2014**, *50*, 1226–1241. [[CrossRef](#)]
63. Temesgen, M.; Rockström, J.; Savenije, H.H.G.; Hoogmoed, W.B.; Alemu, D. Determinants of tillage frequency among smallholder farmers in two semi-arid areas in Ethiopia. *Phys. Chem. Earth Parts A/B/C* **2008**, *33*, 183–191. [[CrossRef](#)]
64. Nachtergaele, F.; van Velthuisen, H.; Verelst, L.; Food and Agriculture Organization of the United Nations (FAO). Harmonized World Soil Database Version 1.2. *Int. Inst. Appl. Syst. Anal. (IIASA), ISRIC-World Soil Information, Inst. Soil Sci. Acad. Sci. (ISSCAS), Jt. Res. Cent. Eur. Comm.* 2012. Available online: <http://www.fao.org/soils-portal/soil-survey/soil-maps-and-databases/harmonized-world-soil-database-v12/en/> (accessed on 21 December 2018).
65. Brunner, M. A National Soil Model of Ethiopia, A Geostatistical Approach to Create a National Soil Map of Ethiopia on the Basis of an SRTM 90 DEM and SOTWIS soil data. Master's Thesis, University of Bern, Bern, Switzerland, 2012.
66. Roth, V.; Lemann, T. Comparing CFSR and conventional weather data for discharge and soil loss modelling with SWAT in small catchments in the Ethiopian Highlands. *Hydrol. Earth Syst. Sci.* **2016**, *20*, 11053–11082. [[CrossRef](#)]
67. Abbaspour, K.C. *SWAT-CUP 2012: SWAT Calibration and Uncertainty Programs—A User Manual*; Swiss Federal Institute of Aquatic Science and Technology: Eawag, Switzerland, 2015.
68. Schuol, J.; Abbaspour, K.C.; Srinivasan, R.; Yang, H. Estimation of freshwater availability in the West African sub-continent using the SWAT hydrologic model. *J. Hydrol.* **2008**, *352*, 30–49. [[CrossRef](#)]
69. Van Griensven, A.; Ndomba, P.; Yalew, S.; Kilonzo, F. Critical review of the application of SWAT in the upper Nile Basin countries. *Hydrol. Earth Syst. Sci.* **2012**, *9*, 3761–3788. [[CrossRef](#)]
70. Van Griensven, A.; Meixner, T.; Grunwald, S.; Bishop, T.; Diluzio, M.; Srinivasan, R. A global sensitivity analysis tool for the parameters of multi-variable catchment models. *J. Hydrol.* **2006**, *324*, 10–23. [[CrossRef](#)]
71. Moriasi, D.N.; Arnold, J.G.; Van Liew, M.W.; Bingner, R.L.; Harmel, R.D.; Veith, T.L. Model evaluation guidelines for systematic quantification of accuracy in watershed simulations. *Trans. ASABE* **2007**, *50*, 885–900. [[CrossRef](#)]
72. Setegn, S.G.; Srinivasan, R.; Dargahi, B. Hydrological Modelling in the Lake Tana Basin, Ethiopia Using SWAT Model. *Open Hydrol. J.* **2008**, *2*, 49–62. [[CrossRef](#)]
73. Krause, P.; Boyle, D.P.; Bäse, F. Comparison of different efficiency criteria for hydrological model assessment. *Adv. Geosci.* **2005**, *5*, 89–97. [[CrossRef](#)]
74. Faramarzi, M.; Abbaspour, K.C.; Ashraf Vaghefi, S.; Farzaneh, M.R.; Zehnder, A.J.B.; Srinivasan, R.; Yang, H. Modeling impacts of climate change on freshwater availability in Africa. *J. Hydrol.* **2013**, *480*, 85–101. [[CrossRef](#)]
75. Schuol, J.; Abbaspour, K.C.; Yang, H.; Srinivasan, R.; Zehnder, A.J.B. Modeling blue and green water availability in Africa. *Water Resour. Res.* **2008**, *44*. [[CrossRef](#)]
76. Engel, B.; Storm, D.; White, M.; Arnold, J.G.; Arabi, M. A Hydrologic/Water Quality Model Application Protocol. *J. Am. Water Resour. Assoc.* **2007**, *43*, 1223–1236. [[CrossRef](#)]
77. Andersen, J.; Refsgaard, J.C.; Jensen, K.H. Distributed hydrological modelling of the Senegal River Basin—Model construction and validation. *J. Hydrol.* **2001**, *247*, 200–214. [[CrossRef](#)]
78. Liu, B.M.; Collick, A.S.; Zeleke, G.; Adgo, E.; Easton, Z.M.; Steenhuis, T.S. Rainfall-discharge relationships for a monsoonal climate in the Ethiopian highlands. *Hydrol. Process.* **2008**, *22*, 1059–1067. [[CrossRef](#)]
79. Steenhuis, T.S.; Hrnčič, M.; Poteau, D.; Romero Luna, E.J.; Tilahun, S.A.; Caballero, L.A.; Guzman, C.D.; Stoof, C.R.; Šanda, M.; Yitaferu, B.; et al. A Saturated Excess Runoff Pedotransfer Function for Vegetated Watersheds. *Vadose Zone J.* **2013**, *12*. [[CrossRef](#)]
80. Hurni, H.; Tato, K.; Zeleke, G. The Implications of Changes in Population, Land Use, and Land Management for Surface Runoff in the Upper Nile Basin Area of Ethiopia. *Mt. Res. Dev.* **2005**, *25*, 147–154. [[CrossRef](#)]
81. Worku, T.; Khare, D.; Tripathi, S.K. Modeling runoff–sediment response to land use/land cover changes using integrated GIS and SWAT model in the Beressa watershed. *Environ. Earth Sci.* **2017**, *76*, 550. [[CrossRef](#)]
82. Karlsson, I.B.; Sonnenborg, T.O.; Refsgaard, J.C.; Trolle, D.; Børgesen, C.D.; Olesen, J.E.; Jeppesen, E.; Jensen, K.H. Combined effects of climate models, hydrological model structures and land use scenarios on hydrological impacts of climate change. *J. Hydrol.* **2016**, *535*, 301–317. [[CrossRef](#)]
83. Teferi, E.; Bewket, W.; Simane, B. Effects of land use and land cover on selected soil quality indicators in the headwater area of the Blue Nile basin of Ethiopia. *Environ. Monit. Assess.* **2016**, *188*, 83. [[CrossRef](#)]

84. Zeleke, G.; Hurni, H. Implications of Land Use and Land Cover Dynamics for Mountain Resource Degradation in the Northwestern Ethiopian Highlands. *Mt. Res. Dev.* **2001**, *21*, 184–191. [[CrossRef](#)]
85. Blume, H.-P.; Brümmer, G.W.; Fleige, H.; Horn, R.; Kandeler, E.; Kögel-Knabner, I.; Kretschmar, R.; Stahr, K.; Wilke, B.-M. *Scheffer/Schachtschabel Soil Science*; Springer Berlin Heidelberg: Berlin, Heidelberg, 2016.
86. Gebrehiwot, S.G.; Gärdenäs, A.I.; Bewket, W.; Seibert, J.; Ilstedt, U.; Bishop, K. The long-term hydrology of East Africa's water tower: Statistical change detection in the watersheds of the Abbay Basin. *Reg. Environ. Chang.* **2014**, *14*, 321–331. [[CrossRef](#)]
87. Beyene, T.; Lettenmaier, D.P.; Kabat, P. Hydrologic impacts of climate change on the Nile River Basin: Implications of the 2007 IPCC scenarios. *Clim. Chang.* **2010**, *100*, 433–461. [[CrossRef](#)]
88. Teklesadik, A.D.; Alemayehu, T.; van Griensven, A.; Kumar, R.; Liersch, S.; Eisner, S.; Tecklenburg, J.; Ewunte, S.; Wang, X. Inter-model comparison of hydrological impacts of climate change on the Upper Blue Nile basin using ensemble of hydrological models and global climate models. *Clim. Chang.* **2017**, *141*, 517–532. [[CrossRef](#)]
89. Adem, A.A.; Tilahun, S.A.; Ayana, E.K.; Worqlul, A.W.; Assefa, T.T.; Dessu, S.B.; Melesse, A.M. Climate Change Impact on Stream Flow in the Upper Gilgel Abay Catchment, Blue Nile basin, Ethiopia. In *Landscape Dynamics, Soils and Hydrological Processes in Varied Climates*; Melesse, A.M., Abtew, W., Eds.; Springer Geography; Springer International Publishing: Cham, Switzerland, 2016; pp. 645–673.
90. Gebre, S.L.; Tadele, K.; Mariam, B.G. Potential Impacts of Climate Change on the Hydrology and Water resources Availability of Didessa Catchment, Blue Nile River Basin, Ethiopia. *J. Geol. Geosci.* **2015**, *4*, 193. [[CrossRef](#)]
91. Taye, M.T.; Willems, P.; Block, P. Implications of climate change on hydrological extremes in the Blue Nile basin: A review. *J. Hydrol. Reg. Stud.* **2015**, *4*, 280–293. [[CrossRef](#)]



© 2018 by the authors. Licensee MDPI, Basel, Switzerland. This article is an open access article distributed under the terms and conditions of the Creative Commons Attribution (CC BY) license (<http://creativecommons.org/licenses/by/4.0/>).